The thin-layer method in a cross-anisotropic 3-D space

Int. J. Numer. Meth. Engng 2012; 89: 537–560

The thin-layer method in a cross-anisotropic 3-D space

by
João Manuel de Oliveira Barbosa[1]
Eduardo Kausel[2]

Abstract

This article presents a generalization of the *Thin-Layer Method* (TLM) to three dimensions, a tool that allows assessing layered media subjected to loads eliciting non-symmetrical wave-fields. It is based on a formulation which fully couples the three components of motion, and allows finding effective solutions to either stationary or moving loads of arbitrary shape that act on —or within— horizontally layered media. In particular, it is an ideal tool for finding analytical solutions to the so-called 2.5D problem, which entails loads with arbitrary distribution in one horizontal coordinate direction together with a harmonic (sinusoidal) variation in the other. Inasmuch as the Green's functions for the latter case are found explicitly in the spatial domain without recourse to numerical integration, it allows using such functions —most likely in the context of the boundary element method (BEM)— as fundamental solutions for problems of soil-structure interaction where the structure is invariant in one horizontal direction, such as a railroad track resting on an embankment. The method entails solving at each frequency of interest two uncoupled eigenvalue problems for generalized SH and SVP waves, after which the fundamental solutions are obtained in closed-form at any desired point in space. Inasmuch as the proposed technique dispenses with at least one of the two inverse Fourier transforms into the spatial domain, in due time the methodology presented is likely to become the preferred tool for a wide class of problems. The technique is first benchmarked against the known solution for a point load and then applied to a rectangular and triangular load distribution.

1. Introduction

The literature on the problem of dynamic loads within homogeneous elastic half-spaces and more generally, of sources acting within layered and/or vertically inhomogeneous media is very rich indeed, and there exist innumerable papers and monographs on the calculation of the wave field elicited by such loads. Besides strictly numerical solutions, such as finite element and finite differences models augmented with absorbing or transmitting boundaries —and more recently, discrete models coupled to perfectly matched layers (PML)— the vast majority of the solution strategies is based on either propagator matrices [1,18], global matrices [15], stiffness matrices [4], or the Thin-Layer Method (TLM) [5,6,9,10,13,14,19]. To the casual reader then, it would seem that there is already a vast arsenal of tools available by means of which one could tackle just about any problem. While there may be some truth to this perception, the fact remains that when one steps up the calculations from two dimensions into three (i.e. attempts to solve problems other than those of plane strain, or with cylindrical symmetry), the computational effort exhibits a substantial jump, which renders even modern computers ineffective for certain classes of problems. For example, a source problem involving time-harmonic line or point loads can be solved effectively by means of a single spatial Fourier or Hankel transform —even if in the case of layered media this may not be a trivial undertaking— whereas non-symmetrical loads, such as

[1] Doctoral Candidate, Department of Civil Engineering, University of Oporto, Portugal. Visiting student at MIT
[2] Professor of Civil and Environmental Engineering, Massachusetts Institute of Technology, Cambridge, MA 02139

rectangular or irregular loads involve two such transforms, which raises enormously the cost and difficulty of the computation and at the very least may render it at impractical. It will be shown that when the TLM is put to the task at hand, it is possible to carry out at least one of the two Fourier transforms in closed form. This reduces the computational effort to that of a series of plane-strain problems supplemented by a numerical transform over the third spatial direction. In other words, the 3D problem is solved as an aggregate of 2D problems of manageable size. To the best of the writers' knowledge, there is no other numerical solution at present possessing these computational advantages.

The TLM is an efficient semi-analytical method for the calculation of the fundamental solutions for layered media. It consists in expressing the displacement field in terms of a finite element expansion in the direction of layering together with analytical descriptions for the remaining directions. In essence, the TLM is a discrete version of the normal modes method familiar to geophysicists, but it differs from it in that the normal modes associated with generalized SH and SVP waves are obtained directly from the solution of two algebraic eigenvalue problems involving narrowly banded matrices, and not by means of search techniques. Thus, the modal superposition involves both the propagating as well as the evanescent modes, which in turn allows accurate computations of the displacement field not only in the distant far field, but also at close distances from the source. At its inception the method was limited to stratified media of finite depth, but when paraxial boundaries became available, they allowed consideration of strata underlain by elastic half-spaces [2,16]. A brief historical account of this method can be found in [10,11]. In the interest of greater generality, the ensuing sections will present the theory for a material which is transversely isotropic (i.e. cross-anisotropic) with respect to horizontal planes.

2. Wave equation in 3-D Cartesian coordinates

Consider a vertically inhomogeneous (or even homogeneous) medium of infinite lateral extent, and at least for now, of arbitrary but finite depth, i.e. a stratum or a plate (to be extended to half-spaces later on). It consists of a linearly elastic material characterized by a mass density ρ and a symmetric constitutive matrix $\mathbf{D} = \{d_{ij}\}$ $(i, j = 1,...,6)$. The medium is subjected to an arbitrary dynamic load $\mathbf{b}$ placed at some location. With dots denoting partial derivatives with respect to time, the dynamic equilibrium equation at a point can be written compactly in matrix format as

$$\rho\ddot{\mathbf{u}} - \mathbf{L}^{\mathrm{T}}\boldsymbol{\sigma} = \mathbf{b} \tag{1}$$

in which the displacement vector $\mathbf{u}$, the stress vector $\boldsymbol{\sigma}$ and the operator matrix $\mathbf{L}$ are defined as

$$\mathbf{u}^{\mathrm{T}} = \{u_x \;\; u_y \;\; u_z\} \tag{2a}$$

$$\boldsymbol{\sigma}^{\mathrm{T}} = \{\sigma_x \;\; \sigma_y \;\; \sigma_z \;\; \tau_{yz} \;\; \tau_{xz} \;\; \tau_{xy}\} \tag{2b}$$

$$\mathbf{L}^{\mathrm{T}} = \begin{bmatrix} \dfrac{\partial}{\partial x} & 0 & 0 & 0 & \dfrac{\partial}{\partial z} & \dfrac{\partial}{\partial y} \\ 0 & \dfrac{\partial}{\partial y} & 0 & \dfrac{\partial}{\partial z} & 0 & \dfrac{\partial}{\partial x} \\ 0 & 0 & \dfrac{\partial}{\partial z} & \dfrac{\partial}{\partial y} & \dfrac{\partial}{\partial x} & 0 \end{bmatrix} \tag{2c}$$

We also consider the stress-strain and the strain-displacement relations

$$\boldsymbol{\sigma} = \mathbf{D}\boldsymbol{\varepsilon} \tag{3a}$$

$$\boldsymbol{\varepsilon} = \mathbf{L}\mathbf{u} \tag{3b}$$

$$\boldsymbol{\varepsilon}^{\mathrm{T}} = \left\{ \varepsilon_x \quad \varepsilon_y \quad \varepsilon_z \quad \gamma_{yz} \quad \gamma_{xz} \quad \gamma_{xy} \right\} \tag{3c}$$

$$\mathbf{D} = \begin{bmatrix} \lambda+2G & \lambda & \lambda_t & 0 & 0 & 0 \\ \lambda & \lambda+2G & \lambda_t & 0 & 0 & 0 \\ \lambda_t & \lambda_t & D_t & 0 & 0 & 0 \\ 0 & 0 & 0 & G_t & 0 & 0 \\ 0 & 0 & 0 & 0 & G_t & 0 \\ 0 & 0 & 0 & 0 & 0 & G \end{bmatrix}, \qquad \begin{matrix} G>0 \\ G_t>0 \\ \lambda+G>0 \\ (\lambda+G)D_t > \lambda_t^2 \end{matrix} \tag{3d}$$

where λ and G are the Lamé constants in the isotropic plane, while λ_t , G_t, D_t are the Lamé constants and the constrained modulus in the transverse direction. The conditions on the right guarantee the positive definiteness of $\mathbf{D}$. When $\lambda_t = \lambda$, $G_t = G$, and $D_t = \lambda + 2G$, the material reduces to an isotropic one. Substituting these expressions into Eq. (1), we are led to the elastic wave equation in 3-D space

$$\rho\ddot{\mathbf{u}} - \mathbf{L}^{\mathrm{T}}\mathbf{D}\mathbf{L}\mathbf{u} = \mathbf{b} \tag{4}$$

On the other hand, the differential operator $\mathbf{L}$ can be expressed as

$$\mathbf{L} = \mathbf{L}_x \frac{\partial}{\partial x} + \mathbf{L}_y \frac{\partial}{\partial y} + \mathbf{L}_z \frac{\partial}{\partial z} \tag{5}$$

in which the coefficient matrices $\mathbf{L}_x, \mathbf{L}_y, \mathbf{L}_z$ are trivially obtained by simple inspection of Eq. (2c). When the medium consists of homogenous layers, the material properties are piecewise constant with depth, in which case the term $\mathbf{L}^{\mathrm{T}}\mathbf{D}\mathbf{L}$ in Eq. (4) can be expanded as

$$\begin{aligned} \mathbf{L}^{\mathrm{T}}\mathbf{D}\mathbf{L} = {} & \mathbf{D}_{xx}\frac{\partial^2}{\partial x^2} + \left(\mathbf{D}_{xy} + \mathbf{D}_{yx}\right)\frac{\partial^2}{\partial x \partial y} + \left(\mathbf{D}_{xz} + \mathbf{D}_{zx}\right)\frac{\partial^2}{\partial x \partial z} \\ & + \mathbf{D}_{yy}\frac{\partial^2}{\partial y^2} + \left(\mathbf{D}_{yz} + \mathbf{D}_{zy}\right)\frac{\partial^2}{\partial y \partial z} + \mathbf{D}_{zz}\frac{\partial^2}{\partial z^2} \end{aligned} \tag{6}$$

with material matrices $\mathbf{D}_{\alpha\beta}$ defined by

$$\mathbf{D}_{\alpha\beta} = \mathbf{L}_a^{\mathrm{T}}\mathbf{D}\mathbf{L}_\beta, \quad \alpha, \beta = x, y, z \tag{7}$$

Tables with the matrices $\mathbf{D}_{\alpha\beta}$ for a cross-anisotropic material are given in Appendix I. On the other hand, the internal stresses in horizontal planes can be obtained as

$$\mathbf{s} = \left\{ \tau_{zx} \quad \tau_{zy} \quad \sigma_z \right\}^{\mathrm{T}} = \mathbf{L}_z^{\mathrm{T}} \boldsymbol{\sigma} = \mathbf{L}_z^{\mathrm{T}} \mathbf{D} \mathbf{L} \mathbf{u} \tag{8}$$

Thus, if one excises out any horizontal slice of the medium and treats it as a free body in space, dynamic equilibrium dictates the need to balance the internal stresses at the now exposed upper and lower surfaces by means of ad hoc external tractions, i.e.

$$\mathbf{T} = \begin{Bmatrix} \mathbf{t}_u \\ \mathbf{t}_l \end{Bmatrix} = \begin{Bmatrix} \mathbf{s}_u \\ -\mathbf{s}_l \end{Bmatrix} \tag{9}$$

where $\mathbf{t}_u$ and $\mathbf{t}_l$ are the external tractions applied at the upper and lower boundaries of the excised domain and $\mathbf{s}_u$ and $\mathbf{s}_l$ the internal stresses at these same locations.

3. Discretization in the vertical direction

We proceed next to discretize the system in the vertical direction, subdividing the medium into horizontal layers which are thin in the finite element sense, i.e. which are small in comparison with the expected wavelengths and strain gradients. Thereafter, we consider an arbitrary thin layer as a free body in space (Figure 1) and express the displacement field within that layer by means of the interpolation ansatz

$$\mathbf{u} = \mathbf{N}\mathbf{U} \tag{10}$$

in which $\mathbf{U} = \mathbf{U}(x, y, \omega)$ is a vector containing the nodal displacements (observe that the "nodes" here are actually horizontal surfaces)

$$\mathbf{U}^{\mathrm{T}} = \left\{ \mathbf{u}_1^{\mathrm{T}} \ \ldots \ \mathbf{u}_m^{\mathrm{T}} \right\}, \quad \mathbf{u}_j^{\mathrm{T}} = \left\{ u_{j,x} \ u_{j,y} \ u_{j,z} \right\}, \qquad j = 1, 2 \cdots m \tag{11}$$

and $\mathbf{N} = \mathbf{N}(z)$ is an interpolation matrix of the form

$$\mathbf{N} = \left[N_1 \mathbf{I} \ \ldots \ N_m \mathbf{I} \right] \tag{12}$$

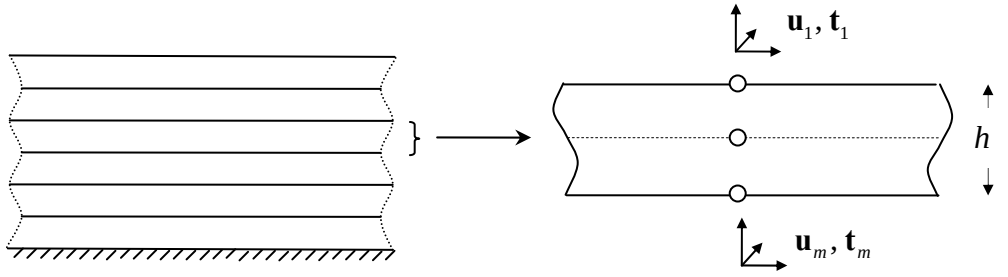

Figure 1: Discretization into thin layers, showing one thin-layer as a free body in space ($m = 3$).

with N_j being the interpolation functions, which depend on the vertical coordinate z. Also, $\mathbf{I}$ is a 3×3 identity matrix, m is the number of nodal surfaces in each thin-layer, and $m-1$ is the interpolation order. When $m > 2$ (i.e. quadratic or cubic thin layers), there exist inner surfaces

which are equidistant from each other. For example, m = 3 corresponds to a quadratic interpolation with one internal nodal surface, as shown in Figure 1, which depicts one thin layer as a free body in space, acted upon and dynamically equilibrated by appropriate tractions applied onto the nodal surfaces.

When we substitute the interpolation (10) into the wave equation (4) and boundary conditions (9), we find that these equations are not satisfied exactly because the ansatz is only an approximation to the actual field, so we find unbalanced body forces $\mathbf{r}$ and boundary tractions $\mathbf{q}$ of the form

$$\mathbf{b} - \rho\ddot{\mathbf{u}} + \mathbf{L}^{\mathrm{T}}\mathbf{D}\mathbf{L}\mathbf{u} = \mathbf{r} \tag{13}$$

$$\begin{Bmatrix} \mathbf{t}_1 \\ \mathbf{t}_m \end{Bmatrix} - \begin{Bmatrix} \mathbf{s}_1 \\ -\mathbf{s}_m \end{Bmatrix} = \begin{Bmatrix} \mathbf{q}_1 \\ \mathbf{q}_m \end{Bmatrix} = \mathbf{q} \tag{14}$$

The discrete wave equation is now obtained by application of the method of the weighted residuals and requiring the virtual work done by the unbalanced forces within the thin-layer and on its bounding surfaces to be zero. This results in the discrete, single thin-layer equation

$$\mathbf{P} = \mathbf{M}\ddot{\mathbf{U}} - \mathbf{A}_{xx}\frac{\partial^2\mathbf{U}}{\partial x^2} - \mathbf{A}_{xy}\frac{\partial^2\mathbf{U}}{\partial x\partial y} - \mathbf{A}_{yy}\frac{\partial^2\mathbf{U}}{\partial y^2} - \mathbf{B}_x\frac{\partial\mathbf{U}}{\partial x} - \mathbf{B}_y\frac{\partial\mathbf{U}}{\partial y} + \mathbf{G}\mathbf{U} \tag{15}$$

where the vector $\mathbf{P}$ contains the consistent external tractions at the interfaces of the thin-layer (which result from the external tractions $\mathbf{t}$ and the body loads $\mathbf{b}$), while the thin-layer matrices $\mathbf{M}$, $\mathbf{A}_{\alpha\beta}$, $\mathbf{B}_\alpha$ and $\mathbf{G}$ are given by

$$\mathbf{M} = \int_0^h \rho\,\mathbf{N}^{\mathrm{T}}\mathbf{N}\,dz \tag{16a}$$

$$\mathbf{A}_{\alpha\alpha} = \int_0^h \mathbf{N}^{\mathrm{T}}\mathbf{D}_{\alpha\alpha}\mathbf{N}^{\mathrm{T}}dz, \quad \alpha = x, y \tag{16b}$$

$$\mathbf{A}_{xy} = \int_0^h \mathbf{N}^{\mathrm{T}}\left(\mathbf{D}_{xy} + \mathbf{D}_{yx}\right)\mathbf{N}\,dz \tag{16c}$$

$$\mathbf{B}_\alpha = \int_0^h \mathbf{N}^{\mathrm{T}}\mathbf{D}_{\alpha z}\mathbf{N}'dz - \int_0^h \mathbf{N}'^{\mathrm{T}}\mathbf{D}_{z\alpha}\mathbf{N}\,dz, \quad \alpha = x, y \tag{16d}$$

$$\mathbf{G} = \int_0^h \mathbf{N}'^{\mathrm{T}}\mathbf{D}_{zz}\mathbf{N}'\,dz \tag{16e}$$

in which h is the thickness of the thin-layer and $\mathbf{N}' = \frac{d}{dz}\mathbf{N}$. Appendix II tabulates the above matrices for an individual thin layer consisting of a cross-anisotropic material and considering both a linear and quadratic interpolation, i.e. $m = 2,3$, respectively. After the individual matrices are overlapped in the usual finite element sense (i.e. layer by layer and in the natural top down order of the interfaces), one is led to a narrowly banded set of global system matrices and vectors which characterize the complete stack of thin layers. The resulting system of partial differential

equations has the same form as Eq. (15), but its shape is now block-tridiagonal and has a correspondingly larger number of equations. To avoid proliferation of symbols, in the ensuing we shall continue to use Eq. (15) as written, but with the implicit understanding that it now refers to the complete assembly of thin layers.

Having obtained the system of equations for a layered system of finite depth, we proceed next to extend it without much ado to layered systems underlain by infinitely deep, homogeneous half-spaces, making use for this purpose of paraxial boundaries attached at the bottommost interface, which together with transition (buffer) layers provide a close approximation to the impedance (dynamic stiffness) of that underlying half-space. Details on these boundaries and their use in the context of the TLM can be found in [2,7,8,16].

4. System equation in wavenumber domain and eigenvalue problem

To solve the system Eq. (15), we proceed to express the displacements **U** and external tractions **P** in the frequency-wavenumber domain, i.e. we carry out the Fourier transformations

$$\bar{\mathbf{U}}\left(k_x,k_y,\omega\right)=\int_{-\infty}^{\infty}\int_{-\infty}^{\infty}\int_{-\infty}^{\infty}\mathbf{U}\left(x,y,t\right)e^{-\mathrm{i}\left(\omega t-k_x x-k_y y\right)}dx\,dy\,dt \tag{17a}$$

$$\bar{\mathbf{P}}\left(k_x,k_y,\omega\right)=\int_{-\infty}^{\infty}\int_{-\infty}^{\infty}\int_{-\infty}^{\infty}\mathbf{P}\left(x,y,t\right)e^{-\mathrm{i}\left(\omega t-k_x x-k_y y\right)}dx\,dy\,dt \tag{17b}$$

after which Eq. (15) changes into

$$\bar{\mathbf{P}}=\left[k_x^2\mathbf{A}_{xx}+k_xk_y\mathbf{A}_{xy}+k_y^2\mathbf{A}_{yy}+\mathrm{i}\left(k_x\mathbf{B}_x+k_y\mathbf{B}_y\right)+\left(\mathbf{G}-\omega^2\mathbf{M}\right)\right]\bar{\mathbf{U}} \tag{18}$$

where $\mathrm{i}=\sqrt{-1}$. All matrices in this expression are symmetric, except for $\mathbf{B}_x$ and $\mathbf{B}_y$ which are skew-symmetric. Although this system could be solved for $\bar{\mathbf{U}}$ as is, it is both possible and convenient to first change the system of equations into a fully symmetric form by means of a *similarity* transformation, which can be shown to preserve all eigenvalues of the characteristic equation. This is accomplished by multiplying every third row of the system (18) by $-\mathrm{i}$ and every third column by i, an operation which solely affects the vectors $\bar{\mathbf{P}}$ and $\bar{\mathbf{U}}$ and the matrices $\mathbf{B}_x$ and $\mathbf{B}_y$, while leaving the other matrices unchanged. As a result of this transformation, the system of equations changes into

$$\tilde{\mathbf{p}}=\left[k_x^2\mathbf{A}_{xx}+k_xk_y\mathbf{A}_{xy}+k_y^2\mathbf{A}_{yy}+k_x\tilde{\mathbf{B}}_x+k_y\tilde{\mathbf{B}}_y+\left(\mathbf{G}-\omega^2\mathbf{M}\right)\right]\tilde{\mathbf{u}} \tag{19}$$

where $\tilde{\mathbf{p}}$ and $\tilde{\mathbf{u}}$ are obtained from $\bar{\mathbf{P}}$ and $\bar{\mathbf{U}}$ by multiplying every third row by $-\mathrm{i}$. Also, $\tilde{\mathbf{B}}_x$ and $\tilde{\mathbf{B}}_y$ are obtained from $\mathbf{B}_x$ and $\mathbf{B}_y$ by simply reversing the sign of every third column [Note: in comparison with previous works on the TLM, we use here a reversed sign for the i factor, for reasons of convenience]. After solving the system of Eq. (19), $\bar{\mathbf{U}}$ is recovered by multiplying every third row of $\tilde{\mathbf{u}}$ by $+\mathrm{i}$, at which time the displacements in the space-time domain can be obtained —at least formally— from the triple inverse Fourier transform

$$\mathbf{U}(x,y,t)=\frac{1}{(2\pi)^3}\int_{-\infty}^{\infty}\int_{-\infty}^{\infty}\int_{-\infty}^{\infty}\bar{\mathbf{U}}(k_x,k_y,\omega)\,e^{\mathrm{i}(\omega t-k_x x-k_y y)}dk_x\,dk_y\,d\omega \tag{20}$$

In the ensuing we shall provide a closed-form solution to the inner inversion of Eq. (20), relying for this purpose on a pair of eigenvalue problems which do *not* depend on the two horizontal wavenumbers k_x, k_y. As a first step in that direction, we begin by re-arranging the order of the degrees of freedom, grouping first all horizontal-*x*, then all horizontal-*y*, and finally all vertical-*z* degrees of freedom. We do this ad-hoc change solely to reveal the special structure possessed by the matrices in Eq. (19) and the implications that this structure has on the eigenvalue problems. Once that task is accomplished, we revert to the usual grouping of degrees of freedom by interface, and not by coordinate direction, to minimize the bandwidth of the equations. After the stated regrouping is accomplished, we find that the matrices attain the following structure:

$$\mathbf{A}_{xx}=\begin{bmatrix}\mathbf{A}_x & \mathbf{O} & \mathbf{O}\\ \mathbf{O} & \mathbf{A}_y & \mathbf{O}\\ \mathbf{O} & \mathbf{O} & \mathbf{A}_z\end{bmatrix},\qquad \mathbf{A}_{yy}=\begin{bmatrix}\mathbf{A}_y & \mathbf{O} & \mathbf{O}\\ \mathbf{O} & \mathbf{A}_x & \mathbf{O}\\ \mathbf{O} & \mathbf{O} & \mathbf{A}_z\end{bmatrix},\qquad \mathbf{A}_{xy}=\begin{bmatrix}\mathbf{O} & \mathbf{A}_x-\mathbf{A}_y & \mathbf{O}\\ \mathbf{A}_x-\mathbf{A}_y & \mathbf{O} & \mathbf{O}\\ \mathbf{O} & \mathbf{O} & \mathbf{O}\end{bmatrix}$$

$$\tilde{\mathbf{B}}_x=\begin{bmatrix}\mathbf{O} & \mathbf{O} & \mathbf{B}\\ \mathbf{O} & \mathbf{O} & \mathbf{O}\\ \mathbf{B}^T & \mathbf{O} & \mathbf{O}\end{bmatrix},\qquad \tilde{\mathbf{B}}_y=\begin{bmatrix}\mathbf{O} & \mathbf{O} & \mathbf{O}\\ \mathbf{O} & \mathbf{O} & \mathbf{B}\\ \mathbf{O} & \mathbf{B}^T & \mathbf{O}\end{bmatrix},\qquad \tilde{\mathbf{u}}=\begin{bmatrix}\mathbf{u}_x\\ \mathbf{u}_y\\ -\mathrm{i}\,\mathbf{u}_z\end{bmatrix}$$

$$\mathbf{G}=\begin{bmatrix}\mathbf{G}_x & \mathbf{O} & \mathbf{O}\\ \mathbf{O} & \mathbf{G}_y & \mathbf{O}\\ \mathbf{O} & \mathbf{O} & \mathbf{G}_z\end{bmatrix},\qquad \mathbf{M}=\begin{bmatrix}\mathbf{M}_x & \mathbf{O} & \mathbf{O}\\ \mathbf{O} & \mathbf{M}_y & \mathbf{O}\\ \mathbf{O} & \mathbf{O} & \mathbf{M}_z\end{bmatrix},\qquad \tilde{\mathbf{p}}=\begin{bmatrix}\mathbf{p}_x\\ \mathbf{p}_y\\ -\mathrm{i}\,\mathbf{p}_z\end{bmatrix} \tag{21}$$

where $\mathbf{O}$ is the null matrix, $\mathbf{G}_x\equiv\mathbf{G}_y$, $\mathbf{M}_x\equiv\mathbf{M}_y\equiv\mathbf{M}_z$. In addition, all sub-matrices are block-tridiagonal and symmetric, except for $\mathbf{B}$ which is not symmetric.

Consider again Eq. (19) and set the right hand side to zero, replace the displacement vector $\tilde{\mathbf{u}}$ by an as yet unknown modal vector $\boldsymbol{\phi}$, and interpret the result as an eigenvalue problem in the two horizontal wavenumbers for some fixed frequency ω:

$$\left(k_x^2\mathbf{A}_{xx}+k_xk_y\mathbf{A}_{xy}+k_y^2\mathbf{A}_{yy}+k_x\tilde{\mathbf{B}}_x+k_y\tilde{\mathbf{B}}_y+\mathbf{G}-\omega^2\mathbf{M}\right)\boldsymbol{\phi}=\mathbf{0} \tag{22}$$

In particular, consider the eigenvalue problem which is obtained by setting $k_y=0$, $k=k_x$. Because of the structure of the matrices, this results in the two *uncoupled* eigenvalue problems

$$\boxed{\left\{k^2\begin{bmatrix}\mathbf{A}_x & \mathbf{O}\\ \mathbf{O} & \mathbf{A}_z\end{bmatrix}+k\begin{bmatrix}\mathbf{O} & \mathbf{B}\\ \mathbf{B}^T & \mathbf{O}\end{bmatrix}+\begin{bmatrix}\mathbf{C}_x & \mathbf{O}\\ \mathbf{O} & \mathbf{C}_z\end{bmatrix}\right\}\begin{bmatrix}\boldsymbol{\phi}_x\\ \boldsymbol{\phi}_z\end{bmatrix}=\begin{bmatrix}\mathbf{0}\\ \mathbf{0}\end{bmatrix}}} \tag{23a}$$

$$\boxed{\left(k^2\mathbf{A}_y+\mathbf{C}_y\right)\boldsymbol{\phi}_y=\mathbf{0}} \tag{23b}$$

where we have used the shorthand

$$\mathbf{C}_x = \mathbf{G}_x - \omega^2 \mathbf{M}_x\,, \qquad \mathbf{C}_y = \mathbf{G}_y - \omega^2 \mathbf{M}_y\,, \qquad \mathbf{C}_z = \mathbf{G}_z - \omega^2 \mathbf{M}_z \tag{24}$$

Eqs. (23a,b) constitute, respectively, the eigenvalue problems for the *normal modes* of generalized Rayleigh (or SVP) and Love (or SH) waves in the stratified medium.

On the other hand, if we set instead $k_x = 0$, $k_y = k$ and consider again the special structure of the matrices given above, we are led once more to the very same two eigenvalue problems, an observation that will allow us to formulate the solution to the full eigenvalue problem in Eq. (22) in terms of the solutions to (23a,b). Indeed, with the polar representation of the wavenumbers

$$k = \sqrt{k_x^2 + k_y^2}\,, \qquad k_x = k\cos\vartheta\,, \qquad k_y = k\sin\vartheta \tag{25}$$

then for any fixed wavenumber direction ϑ, we can show that the eigenvalue problem in Eq. (22) admits eigenvectors of the form

$$\boldsymbol{\phi}_j = \begin{Bmatrix} \boldsymbol{\phi}_{xj}\cos\vartheta \\ \boldsymbol{\phi}_{xj}\sin\vartheta \\ \boldsymbol{\phi}_{zj} \end{Bmatrix} \qquad \text{with} \quad k = k_{Rj} \text{ = eigenvalues of (23a), i.e. Rayleigh modes} \tag{26a}$$

$$\boldsymbol{\phi}_j = \begin{Bmatrix} -\boldsymbol{\phi}_{yj}\sin\vartheta \\ \boldsymbol{\phi}_{yj}\cos\vartheta \\ \mathbf{0} \end{Bmatrix} \qquad \text{with} \quad k = k_{Lj} \text{ = eigenvalues of (23b), i.e. Love modes} \tag{26b}$$

in which j is a modal index whose maximum number (= the number of modes) depends on the number of thin layers, on their expansion order, and on the boundary conditions. The proof of (26a,b) follows by simply substituting these eigenvectors into the expanded form of Eq. (22). For example, substituting the Rayleigh solution (26a), we obtain

$$\begin{aligned}
&\left(k_x^2\mathbf{A}_x + k_y^2\mathbf{A}_y + \mathbf{C}_x\right)\boldsymbol{\phi}_{xj}\cos\vartheta + k_x k_y\left(\mathbf{A}_x - \mathbf{A}_y\right)\boldsymbol{\phi}_{xj}\sin\vartheta + k_x\mathbf{B}\boldsymbol{\phi}_{zj} = \mathbf{0} \\
&k_x k_y\left(\mathbf{A}_x - \mathbf{A}_y\right)\boldsymbol{\phi}_{xj}\cos\vartheta + \left(k_x^2\mathbf{A}_y + k_y^2\mathbf{A}_x + \mathbf{C}_y\right)\boldsymbol{\phi}_{xj}\sin\vartheta + k_y\mathbf{B}\boldsymbol{\phi}_{zj} = \mathbf{0} \\
&k_x\mathbf{B}^T\boldsymbol{\phi}_{xj}\cos\vartheta + k_y\mathbf{B}^T\boldsymbol{\phi}_{xj}\sin\vartheta + \left(\left(k_x^2 + k_y^2\right)\mathbf{A}_z + \mathbf{C}_z\right)\boldsymbol{\phi}_{zj} = \mathbf{0}
\end{aligned} \tag{27}$$

With the polar equivalences for k_x, k_z and identities $\mathbf{C}_x = \mathbf{C}_y$, the above simplifies to

$$\begin{aligned}
&\cos\vartheta\left[\left(k^2\mathbf{A}_x + \mathbf{C}_x\right)\boldsymbol{\phi}_{xj} + k\,\mathbf{B}\boldsymbol{\phi}_{zj}\right] = \mathbf{0} \\
&\sin\vartheta\left[\left(k^2\mathbf{A}_x + \mathbf{C}_x\right)\boldsymbol{\phi}_{xj} + k\,\mathbf{B}\boldsymbol{\phi}_{zj}\right] = \mathbf{0} \\
&k\,\mathbf{B}^T\boldsymbol{\phi}_{xj} + \left(k^2\mathbf{A}_z + \mathbf{C}_z\right)\boldsymbol{\phi}_{zj} = \mathbf{0}
\end{aligned} \tag{28}$$

We observe that the first two are identical to the first equation in (23a), while the third equals the second equation therein. A similar proof applies to the Love modes. Next, we rewrite the

quadratic eigenvalue problem (23a) as a linear eigenvalue problem in k^2, albeit with non-symmetric matrices, so it will admit distinct right and left eigenvectors:

$$\left\{k^2\begin{bmatrix}\mathbf{A}_x & \mathbf{O}\\ \mathbf{B}^T & \mathbf{A}_z\end{bmatrix}+\begin{bmatrix}\mathbf{C}_x & \mathbf{B}\\ \mathbf{O} & \mathbf{C}_z\end{bmatrix}\right\}\begin{bmatrix}\boldsymbol{\phi}_x\\ k\boldsymbol{\phi}_z\end{bmatrix}=\begin{bmatrix}\mathbf{0}\\ \mathbf{0}\end{bmatrix} \qquad \text{Right eigenvectors} \qquad (29a)$$

$$\begin{bmatrix}k\boldsymbol{\phi}_x^T & \boldsymbol{\phi}_z^T\end{bmatrix}\left\{k^2\begin{bmatrix}\mathbf{A}_x & \mathbf{O}\\ \mathbf{B}^T & \mathbf{A}_z\end{bmatrix}+\begin{bmatrix}\mathbf{C}_x & \mathbf{B}\\ \mathbf{O} & \mathbf{C}_z\end{bmatrix}\right\}=\begin{bmatrix}\mathbf{0} & \mathbf{0}\end{bmatrix} \qquad \text{Left eigenvectors} \qquad (29b)$$

With the shorthand $\mathbf{l}^T=\begin{bmatrix}k\boldsymbol{\phi}_x^T & \boldsymbol{\phi}_z^T\end{bmatrix}$ and $\mathbf{r}^T=\begin{bmatrix}\boldsymbol{\phi}_x^T & k\boldsymbol{\phi}_z^T\end{bmatrix}$ for the left and right eigenvectors, respectively, the eigenvalue problem attains the two complementary forms

$$\mathbf{l}_j^T\left(\mathbf{A}k_{Rj}^2+\mathbf{C}\right)=\mathbf{0} \qquad \text{and} \qquad \left(\mathbf{A}k_{Rj}^2+\mathbf{C}\right)\mathbf{r}_j=\mathbf{0} \qquad (30)$$

or in matrix notation

$$\mathbf{K}_R^2\,\mathbf{L}^T\mathbf{A}+\mathbf{L}^T\mathbf{C}=\mathbf{O}, \qquad \mathbf{A}\,\mathbf{R}\,\mathbf{K}_R^2+\mathbf{C}\,\mathbf{R}=\mathbf{O} \qquad (31)$$

where

$$\mathbf{A}=\begin{bmatrix}\mathbf{A}_x & \mathbf{O}\\ \mathbf{B}^T & \mathbf{A}_z\end{bmatrix}, \qquad \mathbf{C}=\begin{bmatrix}\mathbf{C}_x & \mathbf{B}\\ \mathbf{O} & \mathbf{C}_z\end{bmatrix} \qquad (32a)$$

$$\mathbf{L}=\left\{\mathbf{l}_j\right\}=\begin{Bmatrix}\boldsymbol{\Phi}_x\mathbf{K}_R\\ \boldsymbol{\Phi}_z\end{Bmatrix}, \qquad \mathbf{R}=\left\{\mathbf{r}_j\right\}=\begin{Bmatrix}\boldsymbol{\Phi}_x\\ \boldsymbol{\Phi}_z\mathbf{K}_R\end{Bmatrix} \qquad (32b)$$

$$\boldsymbol{\Phi}_x=\left\{\boldsymbol{\phi}_{x1},\boldsymbol{\phi}_{x2},\cdots\right\} \qquad \boldsymbol{\Phi}_z=\left\{\boldsymbol{\phi}_{z1},\boldsymbol{\phi}_{z2},\cdots\right\}, \qquad \mathbf{K}_R=\operatorname{diag}\left\{k_{R1},k_{R2},\cdots\right\} \qquad (32c)$$

The modes in (32b,c) are scaled in such a way that they satisfy the orthogonality conditions

$$\mathbf{L}^T\mathbf{A}\,\mathbf{R}=\mathbf{K}_R, \qquad \mathbf{L}^T\mathbf{C}\,\mathbf{R}=-\mathbf{K}_R^3 \qquad (33)$$

Similarly, the Love wave eigenvalue problem in Eq. (23b) can be written in matrix form as

$$\mathbf{A}_y\boldsymbol{\Phi}_y\mathbf{K}_L^2+\mathbf{C}_y\boldsymbol{\Phi}_y=\mathbf{O}, \qquad \boldsymbol{\Phi}_y=\left\{\boldsymbol{\phi}_{y1},\boldsymbol{\phi}_{y2},\cdots\right\}, \qquad \mathbf{K}_L=\operatorname{diag}\left\{k_{L1},k_{L2},\cdots\right\} \qquad (34)$$

in which the modal matrices satisfy the orthogonality and normalization conditions

$$\boldsymbol{\Phi}_y^T\mathbf{A}_y\boldsymbol{\Phi}_y=\mathbf{I}, \qquad \boldsymbol{\Phi}_y^T\mathbf{C}_y\boldsymbol{\Phi}_y=-\mathbf{K}_L^2 \qquad (35)$$

5. Fundamental solutions in wavenumber domain

We proceed next to combine the eigenvectors for the two eigenvalue problems into one, which leads us to an augmented set of matrices, plus left and right eigenvectors plus orthogonality conditions —compare with Eqs. (26a, 26b, 33, 35):

$$\mathbf{A}=\begin{bmatrix}\mathbf{A}_{xx} & \mathbf{A}_{xy} & \mathbf{O}\\ \mathbf{A}_{xy} & \mathbf{A}_{yy} & \mathbf{O}\\ \mathbf{B}_{xz}^T & \mathbf{B}_{yz}^T & \mathbf{A}_z\end{bmatrix},\qquad \mathbf{C}=\begin{bmatrix}\mathbf{C}_{xx} & \mathbf{O} & \mathbf{B}_{xz}\\ \mathbf{O} & \mathbf{C}_{yy} & \mathbf{B}_{yz}\\ \mathbf{O} & \mathbf{O} & \mathbf{C}_{zz}\end{bmatrix},\qquad \mathbf{K}=\begin{Bmatrix}\mathbf{K}_R & \mathbf{O}\\ \mathbf{O} & \mathbf{K}_L\end{Bmatrix}=\operatorname{diag}\left(k_j\right) \tag{36a}$$

with

$$\left.\begin{aligned}&\mathbf{A}_{xx}=\mathbf{A}_x\cos^2\vartheta+\mathbf{A}_y\sin^2\vartheta && \mathbf{C}_{xx}=\mathbf{C}_{yy}=\mathbf{G}_x-\omega^2\mathbf{M}_x=\mathbf{G}_y-\omega^2\mathbf{M}_y\\ &\mathbf{A}_{yy}=\mathbf{A}_x\sin^2\vartheta+\mathbf{A}_y\cos^2\vartheta && \mathbf{C}_{zz}=\mathbf{G}_z-\omega^2\mathbf{M}_z\\ &\mathbf{A}_{xy}=\left(\mathbf{A}_x-\mathbf{A}_y\right)\sin\vartheta\cos\vartheta && \sin\vartheta=k_y/k\\ &\mathbf{B}_{xz}=\mathbf{B}\cos\vartheta && \cos\vartheta=k_x/k\\ &\mathbf{B}_{yz}=\mathbf{B}\sin\vartheta && k=\sqrt{k_x^2+k_y^2}\end{aligned}\right\} \tag{36b}$$

$$\mathbf{R}=\begin{Bmatrix}\mathbf{\Phi}_x\cos\vartheta & -\mathbf{\Phi}_y\sin\vartheta\\ \mathbf{\Phi}_x\sin\vartheta & \mathbf{\Phi}_y\cos\vartheta\\ \mathbf{\Phi}_z\mathbf{K}_R & \mathbf{O}\end{Bmatrix},\qquad \mathbf{L}=\begin{Bmatrix}\mathbf{\Phi}_x\mathbf{K}_R\cos\vartheta & -\mathbf{\Phi}_y\sin\vartheta\\ \mathbf{\Phi}_x\mathbf{K}_R\sin\vartheta & \mathbf{\Phi}_y\cos\vartheta\\ \mathbf{\Phi}_z & \mathbf{O}\end{Bmatrix} \tag{36c}$$

$$\mathbf{L}^T\mathbf{A}\,\mathbf{R}=\mathbf{J}=\begin{Bmatrix}\mathbf{K}_R & \mathbf{O}\\ \mathbf{O} & \mathbf{I}\end{Bmatrix},\qquad \mathbf{L}^T\mathbf{C}\,\mathbf{R}=-\mathbf{J}\mathbf{K}^2=-\begin{Bmatrix}\mathbf{K}_R^3 & \mathbf{O}\\ \mathbf{O} & \mathbf{K}_L^2\end{Bmatrix} \tag{36d}$$

We are now ready to attempt the inversion of Eq. (19). For this purpose, we first rewrite it as

$$\mathbf{p}^*=\left(\mathbf{A}k^2+\mathbf{C}\right)\mathbf{u}^*,\qquad \mathbf{p}^*=\begin{Bmatrix}\mathbf{p}_x\\ \mathbf{p}_y\\ -\mathrm{i}\,k\,\mathbf{p}_z\end{Bmatrix},\qquad \mathbf{u}^*=\begin{Bmatrix}\mathbf{u}_x\\ \mathbf{u}_y\\ -\mathrm{i}\,k\,\mathbf{u}_z\end{Bmatrix} \tag{37}$$

and proceed to express the displacements in terms of the normal modes, weighted with as yet unknown participation factors $\mathbf{\Gamma}$:

$$\mathbf{u}^*=\mathbf{R}\,\mathbf{\Gamma} \tag{38}$$

Using the orthogonality conditions and solving for the participation factors, we obtain

$$\mathbf{L}^T\mathbf{p}^*=\mathbf{L}^T\left(\mathbf{A}k^2+\mathbf{C}\right)\mathbf{R}\,\mathbf{\Gamma}=\left(\mathbf{L}^T\mathbf{A}\mathbf{R}\,k^2+\mathbf{L}^T\mathbf{C}\mathbf{R}\right)\mathbf{\Gamma}=\mathbf{J}\left(k^2\mathbf{I}-\mathbf{K}^2\right)\mathbf{\Gamma} \tag{39a}$$

$$\mathbf{\Gamma}=\left(k^2\mathbf{I}-\mathbf{K}^2\right)^{-1}\mathbf{J}^{-1}\mathbf{L}^T\mathbf{p}^*=\mathbf{D}\,\mathbf{J}^{-1}\mathbf{L}^T\mathbf{p}^*, \tag{39b}$$

$$\mathbf{D}\equiv\operatorname{diag}\left[D_j\right]=\left(k^2\mathbf{I}-\mathbf{K}^2\right)^{-1}=\operatorname{diag}\left[\frac{1}{k^2-k_j^2}\right] \tag{39c}$$

Hence

$$\mathbf{u}^*=\mathbf{R}\,\mathbf{D}\,\mathbf{J}^{-1}\mathbf{L}^T\mathbf{p}^*,\qquad \mathbf{D}\mathbf{J}^{-1}=\begin{bmatrix}\mathbf{D}_R\mathbf{K}_R^{-1} & \mathbf{O}\\ \mathbf{O} & \mathbf{D}_L\end{bmatrix} \tag{40}$$

or in full

$$\begin{Bmatrix} \mathbf{u}_x \\ \mathbf{u}_y \\ -\mathrm{i}k\,\mathbf{u}_z \end{Bmatrix} = \begin{Bmatrix} \boldsymbol{\Phi}_x \cos\vartheta & -\boldsymbol{\Phi}_y \sin\vartheta \\ \boldsymbol{\Phi}_x \sin\vartheta & \boldsymbol{\Phi}_y \cos\vartheta \\ \boldsymbol{\Phi}_z \mathbf{K}_R & \mathbf{O} \end{Bmatrix} \begin{Bmatrix} \mathbf{D}_R \mathbf{K}_R^{-1} & \mathbf{O} \\ \mathbf{O} & \mathbf{D}_L \end{Bmatrix} \begin{Bmatrix} \mathbf{K}_R \boldsymbol{\Phi}_x^T \cos\vartheta & \mathbf{K}_R \boldsymbol{\Phi}_x^T \sin\vartheta & \boldsymbol{\Phi}_z^T \\ -\boldsymbol{\Phi}_y^T \sin\vartheta & \boldsymbol{\Phi}_y^T \cos\vartheta & \mathbf{O} \end{Bmatrix} \begin{Bmatrix} \mathbf{p}_x \\ \mathbf{p}_y \\ -\mathrm{i}k\,\mathbf{p}_z \end{Bmatrix} \tag{41}$$

Observe that the modal shapes do not depend on the horizontal wavenumbers, i.e. they do not depend on ϑ. Hence, the response in the wavenumber domain is

$$\boxed{\mathbf{u}_x = \boldsymbol{\Phi}_x \mathbf{D}_R \boldsymbol{\Phi}_x^T \left(\mathbf{p}_x \cos^2\vartheta + \mathbf{p}_y \sin\vartheta\cos\vartheta\right) - \mathrm{i}\,\boldsymbol{\Phi}_x \mathbf{D}_R \mathbf{K}_R^{-1} \boldsymbol{\Phi}_z^T \mathbf{p}_z k \cos\vartheta + \boldsymbol{\Phi}_y \mathbf{D}_L \boldsymbol{\Phi}_y^T \left(\mathbf{p}_x \sin^2\vartheta - \mathbf{p}_y \sin\vartheta\cos\vartheta\right)}$$

$$\boxed{\mathbf{u}_y = \boldsymbol{\Phi}_x \mathbf{D}_R \boldsymbol{\Phi}_x^T \left(\mathbf{p}_x \sin\vartheta\cos\vartheta + \mathbf{p}_y \sin^2\vartheta\right) - \mathrm{i}\,\boldsymbol{\Phi}_x \mathbf{D}_R \mathbf{K}_R^{-1} \boldsymbol{\Phi}_z^T \mathbf{p}_z k \sin\vartheta - \boldsymbol{\Phi}_y \mathbf{D}_L \boldsymbol{\Phi}_y^T \left(\mathbf{p}_x \sin\vartheta\cos\vartheta - \mathbf{p}_y \cos^2\vartheta\right)}$$

$$\mathbf{u}_z = \mathrm{i}\tfrac{1}{k} \boldsymbol{\Phi}_z \mathbf{K}_R \mathbf{D}_R \boldsymbol{\Phi}_x^T \left(\mathbf{p}_x \cos\vartheta + \mathbf{p}_y \sin\vartheta\right) + \boldsymbol{\Phi}_z \mathbf{D}_R \boldsymbol{\Phi}_z^T \mathbf{p}_z \tag{42a,b,c}$$

and we have thus succeeded in inverting Eq. (19). Now, as it was already shown in [4, eq. 34], the Rayleigh (SVP) eigenvalue problem satisfies —among several other relationships— the orthogonality condition $\boldsymbol{\Phi}_z \mathbf{K}_R^{-1} \boldsymbol{\Phi}_x^T = \mathbf{O}$. Thus, it follows that

$$\boldsymbol{\Phi}_z \mathbf{K}_R^{-1} \boldsymbol{\Phi}_x^T = \boldsymbol{\Phi}_z \mathbf{D}_R^{-1} \mathbf{D}_R \mathbf{K}_R^{-1} \boldsymbol{\Phi}_x^T = \boldsymbol{\Phi}_z \left(k^2 \mathbf{I} - \mathbf{K}_R^2\right) \mathbf{K}_R^{-1} \mathbf{D}_R \boldsymbol{\Phi}_x^T = k^2 \boldsymbol{\Phi}_z \mathbf{K}_R^{-1} \mathbf{D}_R \boldsymbol{\Phi}_x^T - \boldsymbol{\Phi}_z \mathbf{K}_R \mathbf{D}_R \boldsymbol{\Phi}_x^T = \mathbf{O}$$

so

$$\frac{1}{k} \boldsymbol{\Phi}_z \mathbf{K}_R \mathbf{D}_R \boldsymbol{\Phi}_x^T = k\, \boldsymbol{\Phi}_z \mathbf{K}_R^{-1} \mathbf{D}_R \boldsymbol{\Phi}_x^T$$

which means that (42c) can also be expressed as

$$\boxed{\mathbf{u}_z = \mathrm{i}k\, \boldsymbol{\Phi}_z \mathbf{K}_R^{-1} \mathbf{D}_R \boldsymbol{\Phi}_x^T \left(\mathbf{p}_x \cos\vartheta + \mathbf{p}_y \sin\vartheta\right) + \boldsymbol{\Phi}_z \mathbf{D}_R \boldsymbol{\Phi}_z^T \mathbf{p}_z} \tag{42d}$$

which in most cases is more convenient than (42c).

Table 1: Kernels of fundamental solutions

$$K_{1j} = D_j = \frac{1}{k^2 - k_j^2}, \qquad K_{2j} = D_j \sin\vartheta\cos\vartheta = \frac{k_x k_y}{k^2\left(k^2 - k_j^2\right)}$$

$$K_{3j} = D_j \cos^2\vartheta = \frac{k_x^2}{k^2\left(k^2 - k_j^2\right)}, \qquad K_{4j} = D_j \sin^2\vartheta = \frac{k_y^2}{k^2\left(k^2 - k_j^2\right)}$$

$$K_{5j} = D_j \frac{k}{k_j}\cos\vartheta = \frac{k_x}{k_j\left(k^2 - k_j^2\right)}, \qquad K_{6j} = D_j \frac{k}{k_j}\sin\vartheta = \frac{k_y}{k_j\left(k^2 - k_j^2\right)}$$

$$K_{7j} = D_j \frac{k_j}{k}\cos\vartheta = \frac{k_j k_x}{k^2\left(k^2 - k_j^2\right)}, \qquad K_{8j} = D_j \frac{k_j}{k}\sin\vartheta = \frac{k_j k_y}{k^2\left(k^2 - k_j^2\right)}$$

In the ensuing, it will be implicitly understood that the eigenvalue problem for Rayleigh (SVP) waves will result in eigenvectors $\boldsymbol{\phi}_{xj}$, $\boldsymbol{\phi}_{zj}$ whose components at the m^{th} elevation and j^{th} mode

are written as ϕ_{xj}^m, ϕ_{zj}^m and their eigenvalues are $k_j = k_{Rj}$, while the corresponding eigenvectors $\boldsymbol{\phi}_{yj}$ for Love (SH) waves will have components written as ϕ_{yj}^m with eigenvalues $k_j = k_{Lj}$; this is to conform with the customary symbols used in earlier works on the TLM. Also, in the light of Eq. (39b) and Eq. (42a-d), it is convenient to define the set of *kernels* K_{nj} given in Table 1.

From Eq. (42a-d) and in terms of these kernels, we can express the fundamental solutions $G_{\alpha\beta}^{mn}\left(k_x, k_y, \omega\right)$ at the m^{th} elevation in direction α due to a *unit* load applied at the n^{th} elevation in direction β as listed in Table 2.

Table 2: Fundamental solutions in frequency-wavenumber domain

$$G_{xx}^{mn} = \sum_{j}^{R-\text{modes}} K_{3j}\,\phi_{xj}^m\phi_{xj}^n + \sum_{j}^{L-\text{modes}} K_{4j}\phi_{yj}^m\phi_{yj}^n$$

$$G_{yy}^{mn} = \sum_{j}^{R-\text{modes}} K_{4j}\,\phi_{xj}^m\phi_{xj}^n + \sum_{j}^{L-\text{modes}} K_{3j}\,\phi_{yj}^m\phi_{yj}^n$$

$$G_{xy}^{mn} = \sum_{j}^{R-\text{modes}} K_{2j}\,\phi_{xj}^m\phi_{xj}^n - \sum_{j}^{L-\text{modes}} K_{2j}\,\phi_{yj}^m\phi_{yj}^n = G_{yx}^{mn}$$

$$G_{xz}^{mn} = -\mathrm{i}\sum_{j}^{R-\text{mod}} K_{5j}\,\phi_{xj}^m\phi_{zj}^n\,, \qquad G_{zx}^{mn} = \mathrm{i}\sum_{j}^{R-\text{modes}} K_{7j}\,\phi_{zj}^m\phi_{xj}^n = -G_{xz}^{nm}$$

$$G_{yz}^{mn} = -\mathrm{i}\sum_{j}^{R-\text{modes}} K_{6j}\,\phi_{xj}^m\phi_{zj}^n\,, \qquad G_{zy}^{mn} = \mathrm{i}\sum_{j=1}^{R-\text{modes}} K_{8j}\,\phi_{zj}^m\phi_{xj}^n = -G_{yz}^{nm}$$

$$G_{zz}^{mn} = \sum_{j}^{R-\text{modes}} K_{1j}\,\phi_{zj}^m\phi_{zj}^n$$

6. Inversion of fundamental solutions into the spatial domain

Having obtained the fundamental solutions explicitly in terms of the two horizontal wavenumbers, we now proceed to carry out the inverse Fourier transforms for the displacements elicited by arbitrarily distributed load into the spatial domain. For this purpose, we take advantage of the linearity of the underlying operators, in which case superposition applies. Thus, if $p_\beta\left(k_x, k_y, \omega\right)$ is the Fourier transform of the load in direction $\beta = x, y, z$, then the response functions in direction α at interface m due to that load in direction β applied at interface n, i.e. $u_{\alpha\beta}^{mn}\left(x, y, \omega\right)$, are obtained by replacing in Table 2 the kernels K_{nj} by their inverse Fourier transforms I_{nj}. For example,

$$u_{xx}^{mn}\left(x, y, \omega\right) = \left\{ \sum_{j}^{R-\text{modes}} I_{3j}\,\phi_{xj}^m\phi_{xj}^n + \sum_{j}^{L-\text{modes}} I_{4j}\,\phi_{yj}^m\phi_{yj}^n \right\}, \tag{43}$$

where

$$I_{nj}' = \tfrac{1}{2\pi}\int_{-\infty}^{+\infty} p_\beta\left(k_x, k_y, \omega\right) K_{nj}\, e^{-ik_x x}\, dk_x \tag{44a}$$

$$
\begin{aligned}
I_{nj} &= \tfrac{1}{2\pi}\int_{-\infty}^{+\infty} I'_{nj}\, e^{-ik_y y}\, dk_y \\
&= \left(\tfrac{1}{2\pi}\right)^2 \int_{-\infty}^{+\infty}\int_{-\infty}^{+\infty} p_\beta\left(k_x, k_y, \omega\right) K_{nj}\, e^{-ik_x x} e^{-ik_y y}\, dk_x dk_y
\end{aligned}
\tag{44b}
$$

Of these two inverse transforms, we shall be able to accomplish at least the first one in closed form for various load configurations of engineering interest, and in special cases even both, say for a point load. To verify the correctness of the formulae, we evaluate first the fundamental solutions for point loads, for which the exact expressions in cylindrical coordinates are already available. Thereafter, we present the results for a rectangular load (which exhibits double symmetry, albeit not of the cylindrical kind) and for a triangular load, which is non-symmetric in the y direction.

Table 3: Point load, inverse Fourier transforms in k_x, $\mathrm{Im}\sqrt{k_j^2 - k_y^2} < 0$

$I'_{1j} = \frac{1}{2\pi}\int_{-\infty}^{+\infty} K_{1j}\, \mathrm{e}^{-\mathrm{i}k_x x}\, dk_x$	$= \dfrac{1}{2\mathrm{i}\sqrt{k_j^2 - k_y^2}}\, \mathrm{e}^{-\mathrm{i}\lvert x\rvert\sqrt{k_j^2 - k_y^2}}$
$I'_{2j} = \frac{1}{2\pi}\int_{-\infty}^{+\infty} K_{2j}\, \mathrm{e}^{-\mathrm{i}k_x x}\, dk_x$	$= \dfrac{k_y}{k_j^2}\dfrac{\mathrm{sgn}(x)}{2\mathrm{i}}\left(\mathrm{e}^{-\mathrm{i}\lvert x\rvert\sqrt{k_j^2 - k_y^2}} - \mathrm{e}^{-\lvert k_y x\rvert}\right)$
$I'_{3j} = \frac{1}{2\pi}\int_{-\infty}^{+\infty} K_{3j}\, \mathrm{e}^{-\mathrm{i}k_x x}\, dk_x$	$= \dfrac{1}{2\mathrm{i}k_j^2}\left\{\sqrt{k_j^2 - k_y^2}\, \mathrm{e}^{-\mathrm{i}\lvert x\rvert\sqrt{k_j^2 - k_y^2}} + \mathrm{i}\lvert k_y\rvert \mathrm{e}^{-\lvert k_y x\rvert}\right\}$
$I'_{4j} = \frac{1}{2\pi}\int_{-\infty}^{+\infty} K_{4j}\, \mathrm{e}^{-\mathrm{i}k_x x}\, dk_x$	$= \dfrac{1}{2\mathrm{i}k_j^2}\left\{\dfrac{k_y^2}{\sqrt{k_j^2 - k_y^2}}\mathrm{e}^{-\mathrm{i}\lvert x\rvert\sqrt{k_j^2 - k_y^2}} - \mathrm{i}\lvert k_y\rvert \mathrm{e}^{-\lvert k_y x\rvert}\right\}$
$I'_{5j} = \frac{1}{2\pi}\int_{-\infty}^{+\infty} K_{5j}\, \mathrm{e}^{-\mathrm{i}k_x x}\, dk_x$	$= \dfrac{\mathrm{sgn}(x)}{2\mathrm{i}k_j}\mathrm{e}^{-\mathrm{i}\lvert x\rvert\sqrt{k_j^2 - k_y^2}}$
$I'_{6j} = \frac{1}{2\pi}\int_{-\infty}^{+\infty} K_{6j}\, \mathrm{e}^{-\mathrm{i}k_x x}\, dk_x$	$= \dfrac{k_y}{2\mathrm{i}k_j\sqrt{k_j^2 - k_y^2}}\mathrm{e}^{-\mathrm{i}\lvert x\rvert\sqrt{k_j^2 - k_y^2}}$
$I'_{7j} = \frac{1}{2\pi}\int_{-\infty}^{+\infty} K_{7j}\, \mathrm{e}^{-\mathrm{i}k_x x}\, dk_x$	$= \dfrac{1}{k_j}\dfrac{\mathrm{sgn}(x)}{2\mathrm{i}}\left(\mathrm{e}^{-\mathrm{i}\lvert x\rvert\sqrt{k_j^2 - k_y^2}} - \mathrm{e}^{-\lvert k_y x\rvert}\right)$
$I'_{8j} = \frac{1}{2\pi}\int_{-\infty}^{+\infty} K_{8j}\, \mathrm{e}^{-\mathrm{i}k_x x}\, dk_x$	$= \dfrac{1}{2k_j\mathrm{i}}\left\{\dfrac{k_y}{\sqrt{k_j^2 - k_y^2}}\mathrm{e}^{-\mathrm{i}\lvert x\rvert\sqrt{k_j^2 - k_y^2}} - \mathrm{i}\ \mathrm{sgn}(k_y)\mathrm{e}^{-\lvert k_y x\rvert}\right\}$

a) Point load

As mentioned earlier, for verification purposes we consider first a point load in either the horizontal or vertical direction. In Cartesian coordinates, such a load acting in any horizontal plane would be described simply by $\delta(x)\delta(y)$, the Fourier transform of which is unity (i.e. 1). To carry out the inversion, we begin with the Fourier transform in k_x, assuming throughout that $\mathrm{Im}(k_{Rj}) < 0$, $\mathrm{Im}(k_{Lj}) < 0$, which can be justified by arguing that an infinitesimal amount of damping is always present, which separates the eigenvalues into those that decay in the positive direction and those that decay in the opposite direction, whatever the sign of the real part. After

evaluating the various integrals by means of contour integration in either the lower (for $x>0$) or upper (for $x<0$) complex wavenumber plane k_x, we obtain the formulas given in Table 3, with k_j standing for either the Rayleigh or the Love poles, as may be appropriate. We then go on to evaluate the integral in eq. (44b), which for a point load can also be done in closed form. However, inasmuch as the details of integration are rather lengthy and complicated, they are best relegated to Appendix III. It is found that the inverse Fourier transforms in k_y are as listed in Table 4. These expressions are in agreement with the known formulas for a point load [3], so this confirms the correctness of the current formulation.

Table 4: Point load, inverse Fourier transforms in k_y

$$Z_j = k_j r, \qquad r = \sqrt{x^2 + y^2}, \quad \cos\theta = x/r, \quad \sin\theta = y/r$$

$$I_1 = \frac{1}{4i} H_0^{(2)}\left(Z_j\right)$$

$$I_2 = \frac{\cos\theta\sin\theta}{4\mathrm{i}}\left\{ H_0^{(2)}\left(Z_j\right) - \frac{2}{Z_j}\left(H_1^{(2)}\left(Z_j\right) - \frac{2\mathrm{i}}{\pi Z_j}\right)\right\}$$

$$I_3 = \frac{1}{4i}\left[\cos^2\theta H_0^{(2)}\left(Z_j\right) - \frac{\cos^2\theta - \sin^2\theta}{Z_j}\left(H_1^{(2)}\left(Z_j\right) - \frac{2i}{\pi Z_j}\right)\right]$$

$$I_4 = \frac{1}{4i}\left[\sin^2\theta H_0^{(2)}\left(Z_j\right) + \frac{\cos^2\theta - \sin^2\theta}{Z_j}\left(H_1^{(2)}\left(Z_j\right) - \frac{2i}{\pi Z_j}\right)\right]$$

$$I_5 = -\frac{1}{4}\cos\theta\ H_1^{(2)}\left(Z_j\right), \qquad I_6 = -\frac{1}{4}\sin\theta\ H_1^{(2)}\left(Z_j\right)$$

$$I_7 = -\frac{1}{4}\cos\theta\left(H_1^{(2)}\left(Z_j\right) - \frac{2\mathrm{i}}{\pi Z_j}\right), \qquad I_8 = -\frac{1}{4}\sin\theta\left\{ H_1^{(2)}\left(Z_j\right) - \frac{2\mathrm{i}}{\pi Z_j}\right\}$$

b) Rectangular load

Consider next a uniform rectangular load of dimension $2a\times 2b$ whose sides are parallel to the directions x, y respectively. The load acts either in the horizontal or vertical direction, centered on the vertical axis. The double Fourier transform of the load is

$$p_\beta\left(k_x, k_y\right) = p_{x\beta}\left(k_x\right) p_{y\beta}\left(k_y\right) = \left(\frac{e^{\mathrm{i}k_x a} - e^{-\mathrm{i}k_x a}}{\mathrm{i}\,k_x}\right)\left(\frac{e^{\mathrm{i}k_y b} - e^{-\mathrm{i}k_y b}}{\mathrm{i}\,k_y}\right) = 4\frac{\sin k_x a}{k_x}\frac{\sin k_y b}{k_y} \tag{45}$$

Omitting the term in $p_{y\beta}$, the Fourier inversion in k_x results now in the integrals in Table 5.

Although it is conceivable that the additional transform in k_y for the expressions in Table 5, times $p_{y\beta}$ as defined by Eq. (45), might also be amenable to a closed form solution —a task that we haven't attempted— chances are that it can only be carried out numerically.

Table 5: Rectangular load, integrals in k_x, $\operatorname{Im}\sqrt{k_j^2 - k_y^2} < 0$

$$I'_{nj} = \frac{1}{2\pi}\int_{-\infty}^{+\infty} \frac{e^{-\mathrm{i}k_x(x-a)} - \mathrm{e}^{-\mathrm{i}k_x(x+a)}}{\mathrm{i}k_x} K_{nj}\, dk_x$$

$$I'_1 = \frac{\left(1-\mathrm{e}^{-\mathrm{i}|x+a|\sqrt{k_j^2-k_y^2}}\right)\operatorname{sgn}(x+a) - \left(1-\mathrm{e}^{-\mathrm{i}|x-a|\sqrt{k_j^2-k_y^2}}\right)\operatorname{sgn}(x-a)}{2\left(k_y^2-k_j^2\right)}$$

$$I'_2 = \frac{1}{2k_j^2}\left\{\frac{k_y}{\sqrt{k_j^2-k_y^2}}\left(\mathrm{e}^{-\mathrm{i}|x+a|\sqrt{k_j^2-k_y^2}} - \mathrm{e}^{-\mathrm{i}|x-a|\sqrt{k_j^2-k_y^2}}\right) - \mathrm{i}\,\operatorname{sgn}(k_y)\left(\mathrm{e}^{-|k_y(x+a)|} - \mathrm{e}^{-|k_y(x-a)|}\right)\right\}$$

$$I'_3 = \frac{1}{2k_j^2}\left\{\left(\mathrm{e}^{-|k_y(x-a)|} - \mathrm{e}^{-\mathrm{i}|x-a|\sqrt{k_j^2-k_y^2}}\right)\operatorname{sgn}(x-a) - \left(\mathrm{e}^{-|k_y(x+a)|} - \mathrm{e}^{-\mathrm{i}|x+a|\sqrt{k_j^2-k_y^2}}\right)\operatorname{sgn}(x+a)\right\}$$

$$I'_4 = \frac{1}{2k_j^2}\left\{\left(\frac{k_y^2}{k_y^2-k_j^2}\left(1-e^{-i\sqrt{k_j^2-k_y^2}\,|x+a|}\right) - \left(1-e^{-|k_y(x+a)|}\right)\right)\operatorname{sgn}(x+a)\right.$$
$$\left. - \left(\frac{k_y^2}{k_y^2-k_j^2}\left(1-e^{-i\sqrt{k_j^2-k_y^2}\,|x-a|}\right) - \left(1-e^{-|k_y(x-a)|}\right)\right)\operatorname{sgn}(x-a)\right\}$$

$$I'_5 = \frac{1}{2\,k_j\sqrt{k_j^2-k_y^2}}\left(\mathrm{e}^{-\mathrm{i}\sqrt{k_j^2-k_y^2}\,|x+a|} - \mathrm{e}^{-\mathrm{i}\sqrt{k_j^2-k_y^2}\,|x-a|}\right)$$

$$I'_6 = \frac{k_y}{2k_j\left(k_y^2-k_j^2\right)}\left(\left(1-\mathrm{e}^{-\mathrm{i}\sqrt{k_j^2-k_y^2}\,|x+a|}\right)\operatorname{sgn}(x+a) - \left(1-\mathrm{e}^{-\mathrm{i}\sqrt{k_j^2-k_y^2}\,|x-a|}\right)\operatorname{sgn}(x-a)\right)$$

$$I'_7 = \frac{1}{2k_j}\left(\frac{1}{\sqrt{k_j^2-k_y^2}}\left(\mathrm{e}^{-\mathrm{i}\sqrt{k_j^2-k_y^2}|x+a|} - \mathrm{e}^{-\mathrm{i}\sqrt{k_j^2-k_y^2}|x-a|}\right) + \frac{1}{\mathrm{i}|k_y|}\left(\mathrm{e}^{-|k_y(x+a)|} - \mathrm{e}^{-|k_y(x-a)|}\right)\right)$$

$$I'_8 = \frac{1}{2k_y\,k_j}\left\{\operatorname{sgn}(x-a)\left(1+e^{-|k_y(x-a)|} - \frac{k_y^2}{k_y^2-k_j^2}\left(1-e^{-i\sqrt{k_j^2-k_y^2}|x-a|}\right)\right)\right.$$
$$\left. - \operatorname{sgn}(x+a)\left(1+e^{-|k_y(x+a)|} - \frac{k_y^2}{k_y^2-k_j^2}\left(1-e^{-i\sqrt{k_j^2-k_y^2}|x+a|}\right)\right)\right\}$$

c) Triangular load

Consider next the uniform triangular load shown in Figure 2.

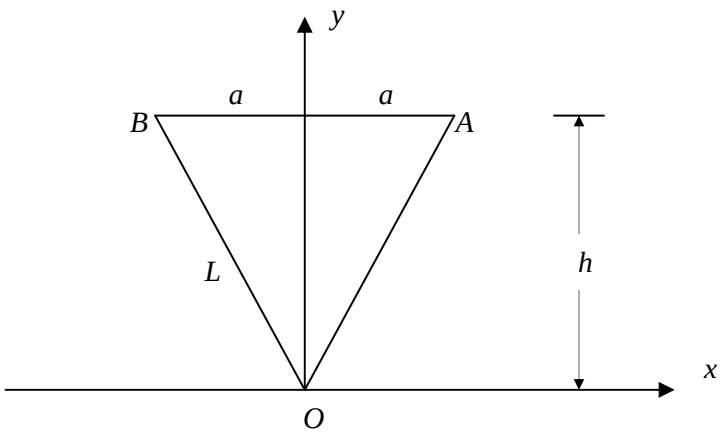

Figure 2: Triangular load

The wavenumber content of such load can be shown to be given by

$$\tilde{P}\left(k_x,k_y\right)=\iint_A e^{\mathrm{i}k_x x}e^{\mathrm{i}k_y y}dA=\frac{h}{k_x}\left[\frac{1-e^{i\left(k_y h+k_x a\right)}}{k_y h+k_x a}-\frac{1-e^{i\left(k_y h-k_x a\right)}}{k_y h-k_x a}\right] \tag{46}$$

In the ensuing, we shall use the symbol $\bar{x}$ as a dummy function argument which will stand for either x, $x-a$ or $x+a$. Also, we shall use a sub-index $\pm$ to denote the optional sign of certain arguments. The evaluation of the inverse Fourier transforms in k_x can be accomplished using contour integration in an appropriate complex half-plane, a somewhat tedious process which requires finding the residues of the various poles of the integrand while accounting properly for the signs of x and $x\pm a$ as well as the sign of k_y. For example, the first integral has poles at $k_x=\pm k_y h/a$ and $k_x=\pm\sqrt{k_j^2-k_y^2}$. After this is done, the inverse Fourier transforms are found to be as follows:

$$\boxed{I'_{nj}=h\left[I_{n+}\left(x\right)-I_{n-}\left(x\right)-e^{i\,k_y h}I_{n+}\left(x-a\right)+e^{i\,k_y h}I_{n-}\left(x+a\right)\right]},\qquad n=1,2\cdots 8 \tag{47}$$

for which the requisite integrals are given in Table 6 (using numerical integration, we have verified that these formulas are correct).

Table 6: Triangular load, auxiliary integrals over k_x, $\mathrm{Im}\sqrt{k_j^2-k_y^2}<0$

$$I_{1\pm}(\bar{x})=\mathrm{i}\frac{\mathrm{sgn}(\bar{x})}{2}a^2\left[\frac{1}{k_y h}\left(\frac{e^{\pm i\frac{k_y h}{a}\bar{x}}}{k_y^2h^2+\left(k_y^2-k_j^2\right)a^2}-\frac{1}{\left(k_y^2-k_j^2\right)a^2}\right)+\frac{\mathrm{e}^{-\mathrm{i}\sqrt{k_j^2-k_y^2}|\bar{x}|}}{\left(k_y^2-k_j^2\right)a^2\left[k_y h\pm\mathrm{sgn}(\bar{x})a\sqrt{k_j^2-k_y^2}\right]}\right]$$

$$I_{2\pm}(\bar{x})=-\mathrm{i}\frac{1}{2k_j^2}\left[\pm\frac{\left(k_j a\right)^2}{k_y h}\frac{\mathrm{e}^{\pm\mathrm{i}\frac{k_y h}{a}\bar{x}}}{k_y^2h^2+\left(k_y^2-k_j^2\right)a^2}\left(\frac{ha}{h^2+a^2}\right)\mathrm{sgn}(\bar{x})\right.$$
$$\left.+\frac{k_y h\,\mathrm{e}^{-\mathrm{i}\sqrt{k_j^2-k_y^2}|\bar{x}|}}{a\sqrt{k_j^2-k_y^2}\left[k_y h\pm\mathrm{sgn}(\bar{x})a\sqrt{k_j^2-k_y^2}\right]}\left(\frac{a}{h}\right)+\frac{\mathrm{sgn}(k_y)\mathrm{e}^{-|k_y\bar{x}|}}{\mathrm{i}\left[k_y h\mp\mathrm{i}\,\mathrm{sgn}(\bar{x})|k_y|a\right]}\right]$$

$$I_{3\pm}(\bar{x})=\mathrm{i}\frac{\mathrm{sgn}(\bar{x})}{2k_j^2}\left[\frac{\left(k_j a\right)^2}{k_y h}\frac{\mathrm{e}^{\pm\mathrm{i}\frac{k_y h}{a}\bar{x}}}{k_y^2h^2+\left(k_y^2-k_j^2\right)a^2}\left(\frac{h^2}{h^2+a^2}\right)\right.$$
$$\left.+\frac{\mathrm{e}^{-|k_y\bar{x}|}}{k_y h\mp\mathrm{i}\,\mathrm{sgn}(\bar{x})a|k_y|}-\frac{\mathrm{e}^{-\mathrm{i}\sqrt{k_j^2-k_y^2}|\bar{x}|}}{k_y h\pm\mathrm{sgn}(\bar{x})a\sqrt{k_j^2-k_y^2}}\right]$$

$$I_{4\pm}(\bar{x})=\mathrm{i}\frac{\mathrm{sgn}(\bar{x})}{2k_j^2}\left[\frac{\left(k_j a\right)^2}{k_y h}\left(\frac{\mathrm{e}^{\pm\mathrm{i}\frac{k_y h}{a}\bar{x}}}{\left(k_y h\right)^2+\left(k_y^2-k_j^2\right)a^2}\left(\frac{a^2}{h^2+a^2}\right)-\frac{1}{\left(k_y^2-k_j^2\right)a^2}\right)\right.$$
$$\left.+\frac{\left(k_y h\right)^2\mathrm{e}^{-\mathrm{i}\sqrt{k_j^2-k_y^2}|\bar{x}|}}{\left(k_y^2-k_j^2\right)a^2\left[k_y h\pm\mathrm{sgn}(\bar{x})a\sqrt{k_j^2-k_y^2}\right]}\left(\frac{a}{h}\right)^2-\frac{\mathrm{e}^{-|k_y\bar{x}|}}{k_y h\mp\mathrm{i}\,\mathrm{sgn}(\bar{x})|k_y|a}\right]$$

$$I_{5\pm}(\bar{x})=-\mathrm{i}\frac{a}{2k_j}\left[\pm\frac{\mathrm{sgn}(\bar{x})\mathrm{e}^{\pm\mathrm{i}\frac{k_y h}{a}\bar{x}}}{\left(k_y h\right)^2+\left(k_y^2-k_j^2\right)a^2}+\frac{\mathrm{e}^{-\mathrm{i}\sqrt{k_j^2-k_y^2}|\bar{x}|}}{a\sqrt{k_j^2-k_y^2}\left[k_y h\pm\mathrm{sgn}(\bar{x})a\sqrt{k_j^2-k_y^2}\right]}\right]$$

$$I_{6\pm}(\bar{x})=\mathrm{i}\frac{\mathrm{sgn}(\bar{x})}{2}\frac{a^2}{k_j h}\left[\frac{e^{\pm i\frac{k_y h}{a}\bar{x}}}{\left(k_y h\right)^2+\left(k_y^2-k_j^2\right)a^2}-\frac{1}{\left(k_y^2-k_j^2\right)a^2}+\frac{k_y h e^{-i\sqrt{k_j^2-k_y^2}|\bar{x}|}}{\left(k_y^2-k_j^2\right)a^2\left[k_y h\pm\mathrm{sgn}(\bar{x})a\sqrt{k_j^2-k_y^2}\right]}\right]$$

$$I_{7\pm}(\bar{x}) = -\mathrm{i}\frac{a}{2k_j}\left[\pm\left(\frac{k_j a}{k_y h}\right)^2 \frac{\operatorname{sgn}(\bar{x})\, e^{\pm i\frac{k_y h}{a}\bar{x}}}{k_y^2 h^2 + \left(k_y^2 - k_j^2\right)a^2}\left(\frac{h^2}{h^2+a^2}\right)\right.$$

$$\left. + \frac{e^{-i\sqrt{k_j^2-k_y^2}|\bar{x}|}}{a\sqrt{k_j^2-k_y^2}\left[k_y h \pm \operatorname{sgn}(\bar{x})\, a\sqrt{k_j^2-k_y^2}\right]} + \frac{e^{-|k_y\bar{x}|}}{\mathrm{i}\,|k_y h|\left[k_y h \mp \mathrm{i}\operatorname{sgn}(\bar{x})|k_y|\, a\right]}\left(\frac{h}{a}\right)\right]$$

$$I_{8\pm}(\bar{x}) = \mathrm{i}\frac{\operatorname{sgn}(\bar{x})\, h}{2k_j}\left[\frac{k_j^2 a^2}{k_y^2 h^2\left(k_j^2 - k_y^2\right)a^2} + \frac{k_j^2 a^2\, \mathrm{e}^{\pm\mathrm{i}\frac{k_y h}{a}\bar{x}}}{k_y^2 h^2\left[k_y^2 h^2 + \left(k_y^2 - k_j^2\right)a^2\right]}\frac{a^2}{h^2+a^2}\right.$$

$$\left. + \frac{k_y h\, \mathrm{e}^{-\mathrm{i}\sqrt{k_j^2-k_y^2}|\bar{x}|}}{\left(k_y^2 - k_j^2\right)a^2\left[k_y h \pm \operatorname{sgn}(\bar{x})\, a\sqrt{k_j^2-k_y^2}\right]}\frac{a^2}{h^2} - \frac{\mathrm{e}^{-|k_y\bar{x}|}}{k_y h\left[k_y h \mp \mathrm{i}\,\operatorname{sgn}(\bar{x})|k_y|\, a\right]}\right]$$

7. Examples of application

We proceed to demonstrate the method described herein by means of three numerical examples. The first is for validation purposes, and deals with the response to a point load of a homogeneous full-space in (x, k_y, z, ω) domain, for which a closed form solution exists. The second and third examples also deal with a full space, but this time subjected to distributed square and triangular loads, which are compared against the results obtained by numerical integration of the exact point load solution available in the literature [12].

a) Harmonic line load in a homogeneous full-space

Consider an isotropic full-space with mass density $\rho = 1$, shear modulus $G = 1$ and Poisson's ratio $\nu = 0.25$, subjected to a time harmonic line load $\mathbf{b}(x, y, z, t) = \delta(x)\delta(z)\exp(\mathrm{i}\omega t - \mathrm{i}k_y y)$. The exact solution to this problem in the (x, k_y, z, ω) domain can be found in [12, 17]. Here, we compute the displacements in the horizontal plane $z = 0$ at horizontal distances $x = 0.01\lambda$, $x = \lambda$ and $x = 5\lambda$ for a line load applied at the origin with excitation frequency $f = 1$ Hz i.e. $\omega = 2\pi$. The reference wavelength for this example is $\lambda = C_S / f = 1$, where $C_S = \sqrt{G/\rho} = 1$ is the shear wave velocity.

To avoid discretization effects —about which a discussion can be found in [11]— the full-space is modeled with an elastic layer with thickness 20m, subdivided into 200 thin-layers with a quadratic expansion, which is supplemented by means of paraxial boundaries at its upper and lower horizons that simulate the infinite extent of the medium. This gives about 10 quadratic thin-layers per wavelength, which is more than enough to obtain accurate results. Also, inasmuch

as the exact solution is singular under the load yet it is finite in the discrete solution, we place the closest receiver at $x = 0.01\lambda$. In the TLM model, the load is applied at the middle surface. To avoid strong oscillations in the response, a small amount of damping $\xi_P = \xi_S = 0.005$ is added, which renders the wave velocities complex. Figures 3a, 2b and 3c depict a comparison of the vertical displacements due to a vertical load obtained by the current procedure and by the analytical solution.

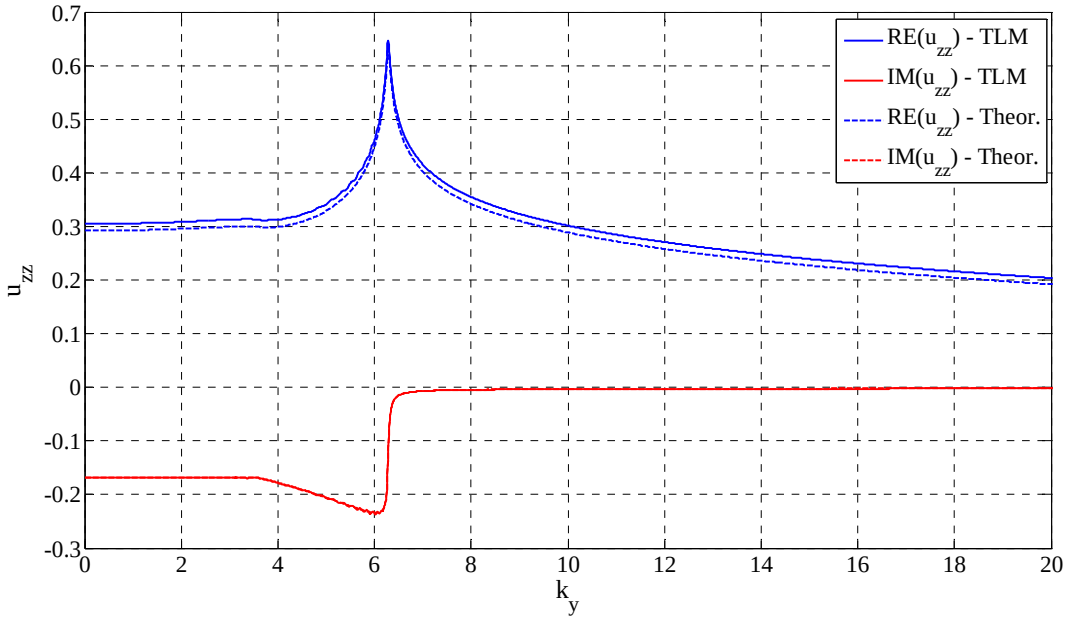

Figure 3a: Displacements at $x = 0.01\lambda$

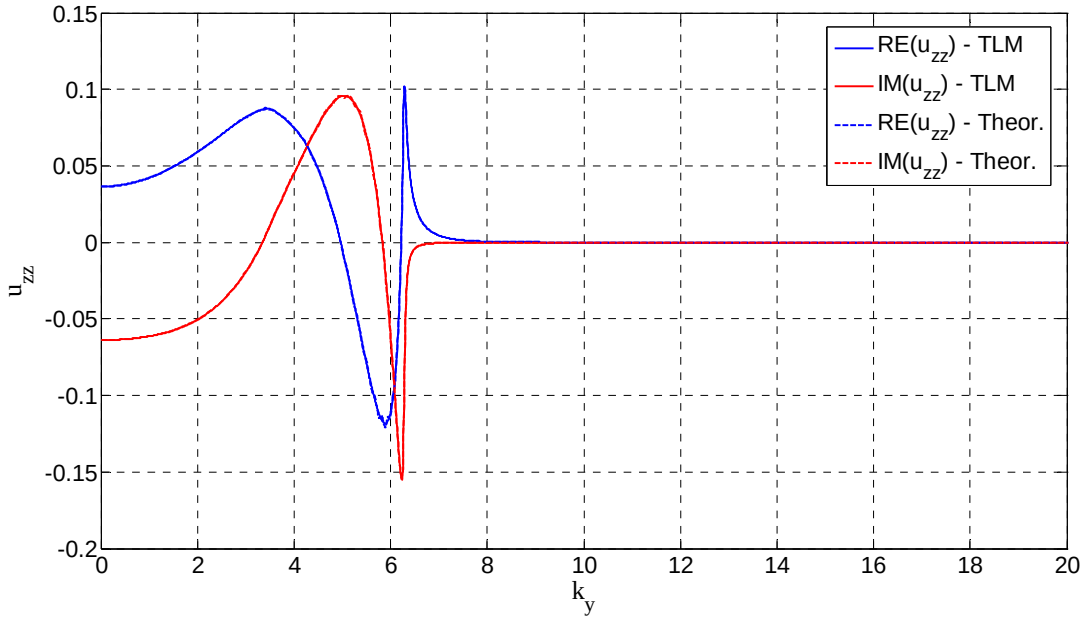

Figure 3b: Displacements at $x = \lambda$

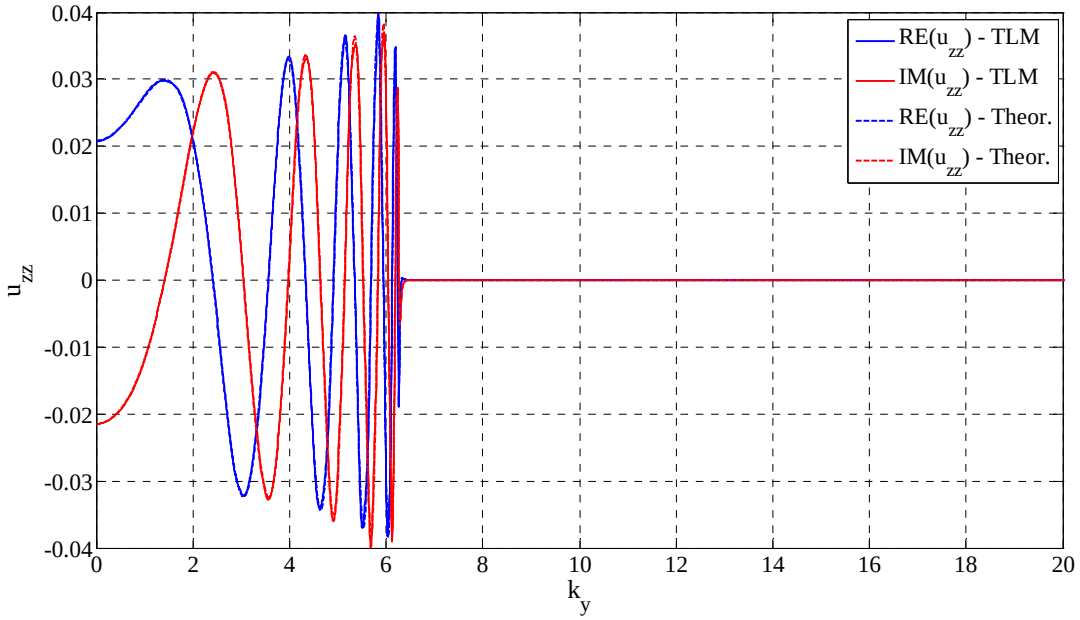

Figure 3c: Displacements at $x = 5\lambda$

As can be seen from Figures 3b and 3c, the match between the exact solution and the TLM solution is supremely good, to the point that one can hardly distinguish between the two results. Nonetheless, very near the load (Figure 3a) one can observe a rather small difference in the real part which is due to discretization effects. This is because the thickness of the thin layers is only 0.1λ while the receiver is placed at one tenth of that distance from the source. Still, given the excellent quality of the comparison even at that short range, this demonstrates the robustness of the TLM solution, especially in the light of the paraxial boundaries being used.

Observe that at large distances the response decays very fast with the wavenumber k_y beyond the threshold $k_S = \omega / C_S$ (the branch point), while below that value the response is highly wavy. Hence, when computing the inverse transform from k_y–space into *y*–space for remote points, one can truncate the integrals at the branch point; but then again because of the rapid oscillations one must consider a sufficiently dense number of points below that threshold. Conversely, for receivers at close range, the response functions are less wavy, but they also decay more slowly with k_y. Hence, their Fourier inversion must include points beyond the branch point even if one can get away with coarser spacing.

b) Square load within a homogeneous full-space

Consider again the full-space of the previous example, but now acted upon in the $z = 0$ plane by a square load of size $\lambda \times \lambda$ acting in the *y* direction. Using the same model as in the previous example, we determine the displacements in the *y* direction for receivers placed in the plane $z = 0$ at ranges $x = 0$ (axis), $x = \frac{1}{2}\lambda$ (edge of load) and $x = 5\lambda$. The displacements obtained with the TLM are compared with the results obtained by integrating the exact point load solution [12] over the loaded area. Figures 4a-c show on the left the transfer function in k_y (i.e. before multiplication by the load spectrum) and on the right the displacements obtained by the two different approaches.

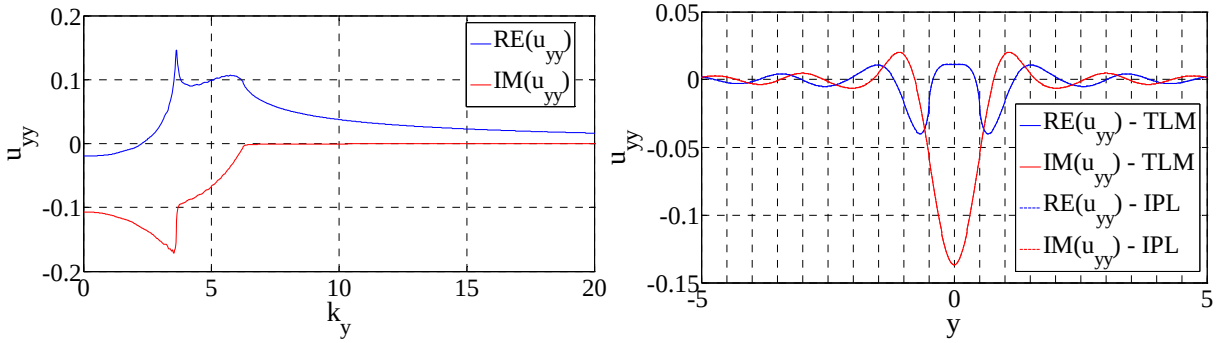

Figure 4a: Transfer function (left) and displacements in space domain (right), $x = 0$

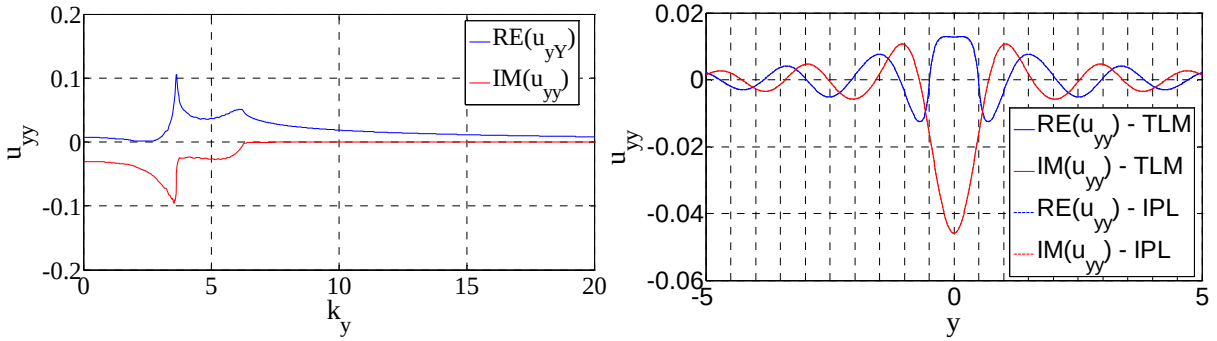

Figure 4b: Transfer function (left) and displacements in space domain (right), $x = \frac{1}{2}\lambda$

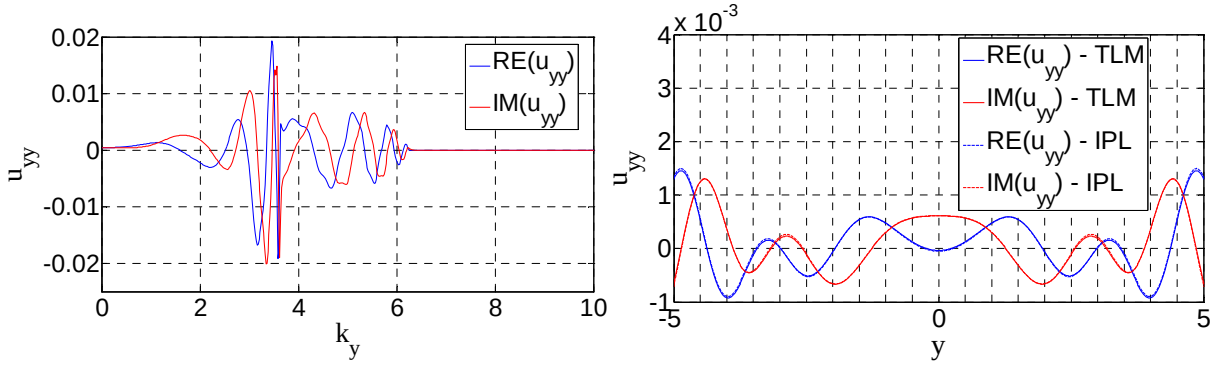

Figure 4c: Transfer function (left) and displacements in space domain (right), $x = 5\lambda$

From Figs. 4a-c we observe once more that the displacements obtained with the TLM are in excellent agreement with those obtained by numerical integration of the exact point load solution. Again, the transfer functions for receivers close to the load decay more slowly with k_y, but are also less wavy than the functions for remote receivers, and these effects dictate the number of integration points in k_y needed. We emphasize that it is not necessary to repeat the calculation of the eigenvalue problems as k_y is changed.

c) Triangular load within a homogeneous full-space

Finally, we repeat the steps of the previous example, but this time considering a triangular load with height and base $h = 2a = \lambda$, see Figure 2, and again we compute the response both with the TLM and by numerical integration of the exact solution. The displacements in x elicited by a

load in x are shown in Figures 5a-c as function of y, for receivers with ranges $x=0$, $x=\frac{1}{2}\lambda$ (corner of triangle) and $x=5\lambda$ (far field). This time the load is not symmetric in y, so the wavenumber spectrum of the load in k_y is not symmetric either, which means that we must also calculate the displacements for negative wavenumbers.

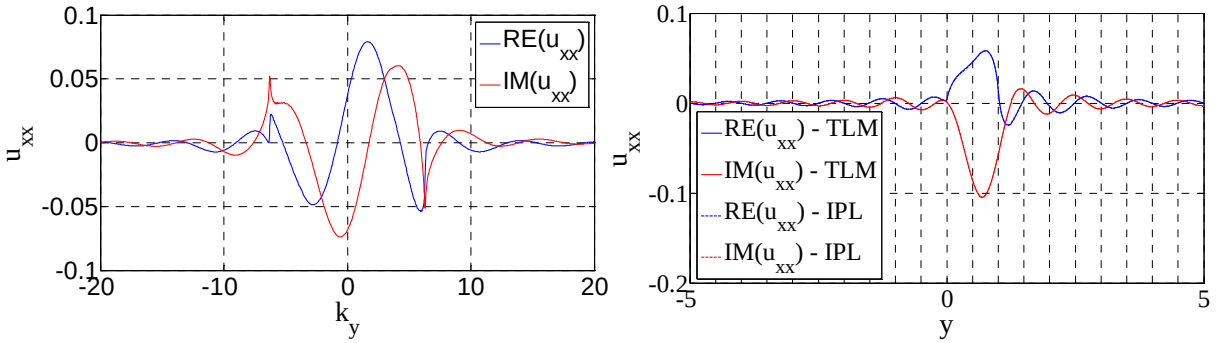

Figure 5a: Transfer function (left) and displacements in space domain (right), $x=0$

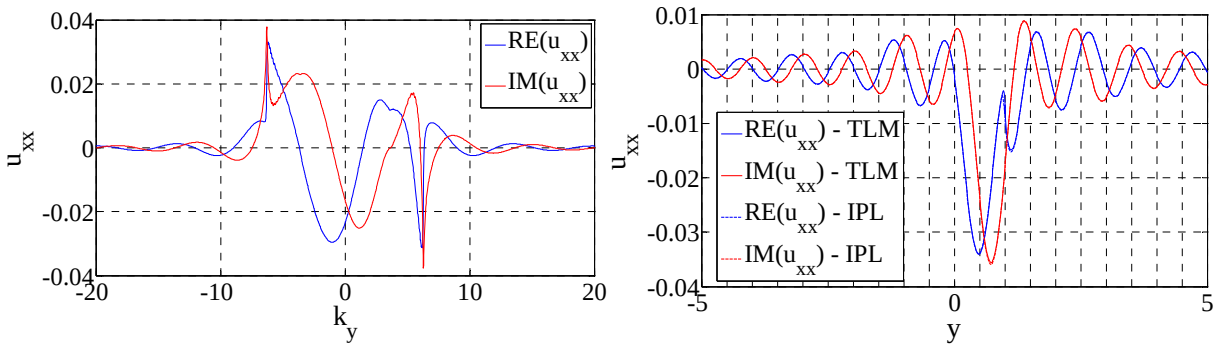

Figure 5b: Transfer function (left) and displacements in space domain (right), $x=\frac{1}{2}\lambda$

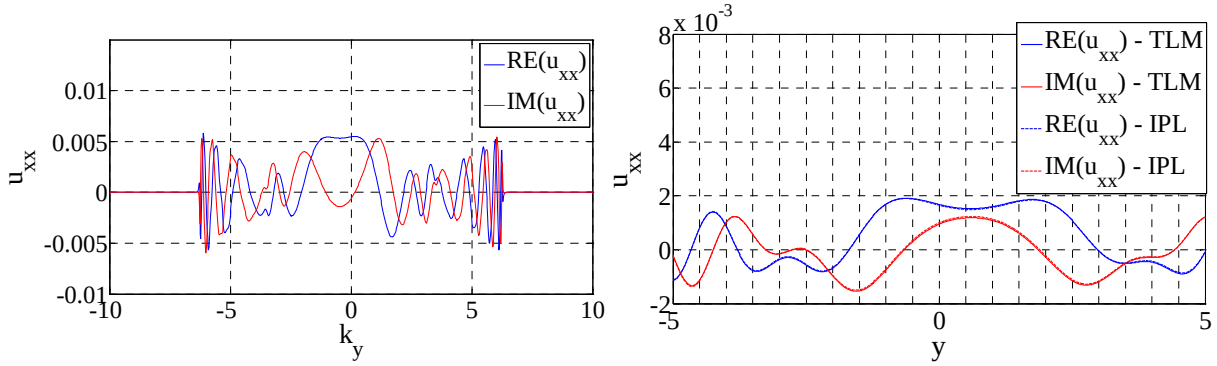

Figure 5c: Transfer function (left) and displacements in space domain (right), $x=5\lambda$

Figures 5a-c demonstrate yet again an excellent agreement between the two approaches. Also, in Figure 5b we observe a discontinuity of the displacement in the vicinity of $y=\lambda$, which corresponds to the corner of the triangle. In Figure 5c we can see that the displacements are almost symmetric with respect to $y=0.66\lambda$, which corresponds to the center of gravity of the load.

8. Conclusions

This article presented a generalization of the Thin-Layer Method (TLM) into a three-dimensional, cross-anisotropic space for dynamic loads in layered media in which loads and displacements exhibit neither plane strain nor cylindrical symmetry. In general, the previously available numerical solutions for problems of this nature called for numerically intensive, double Fourier transforms in the two horizontal wavenumbers, which we may refer to as the longitudinal (x) and transverse (y) wavenumbers. The technique presented herein, however, circumvents much of that effort by being able to carry out at least one of those two transforms in closed form. Like the standard TLM formulation in plane strain and cylindrical geometry, the technique herein relies on the solution of two eigenvalue problems for generalized Rayleigh and Love waves, but inasmuch as these eigenvalue problems need not be repeated for each transverse wavenumber, the Fourier inversion in the remaining direction can be carried out very efficiently. Furthermore, this can be done for any range x, inasmuch as the transfer functions in x, k_y, z, ω are already available everywhere. The technique is so efficient that we believe that in due time it will be regarded as the method of choice for this class of problems. In a companion paper to be submitted separately, the writers will apply the described algorithm to moving loads of arbitrary shape, obtaining results in the time domain by means of a single Fourier transform.

If the examples presented were all for a full, homogeneous space it is because for that environment there exist *exact* solutions which can be used as benchmarks against which to assess the numerical solutions. In addition, the very close fit attained with the benchmarks demonstrated also the quality of the paraxial approximations used to model the infinite medium. It should be very clearly understood, however, that the computational effort and accuracy of the proposed technique will remain exactly the same if the medium had been chosen to be layered and consisting of transversely isotropic materials, or if the medium had been "simply" a half-space, layered or not. In these cases, however, we no longer have reference solutions available for comparison. However, the efficiency of the algorithm does not at all depend on the heterogeneity in the vertical direction, i.e. in the direction of layering.

9. Acknowledgement

The first author wishes to thank the financial support he received from the *Fundação para a Ciência e a Tecnologia* of Portugal (FCT) through grant number SFRH/BD/47724/2008 and from the *Risk Assessment and Management for High-Speed Rail Systems*' project of the MIT—Portugal Program in the Transportation Systems Area. He also wishes to thank his academic advisors Prof. Rui Calçada and Prof. Álvaro Azevedo of the University of Oporto for arranging his traineeship at MIT as a visiting student under the umbrella of the MIT-Portugal Program.

Appendix I – Matrices $\mathbf{D}_{\alpha\beta}$ for cross-anisotropic materials

With the constitutive matrix **D** defined by Eq. (3d), the matrices $\mathbf{D}_{\alpha\beta}$ in Eq. (7) are

$$\mathbf{D}_{xx}=\begin{bmatrix}\lambda+2G & 0 & 0\\ 0 & G & 0\\ 0 & 0 & G_t\end{bmatrix};\qquad \mathbf{D}_{xy}=\begin{bmatrix}0 & \lambda & 0\\ G & 0 & 0\\ 0 & 0 & 0\end{bmatrix};\qquad \mathbf{D}_{xz}=\begin{bmatrix}0 & 0 & \lambda_t\\ 0 & 0 & 0\\ G_t & 0 & 0\end{bmatrix}$$

$$\mathbf{D}_{yx}=\begin{bmatrix}0 & G & 0\\ \lambda & 0 & 0\\ 0 & 0 & 0\end{bmatrix};\qquad \mathbf{D}_{yy}=\begin{bmatrix}G & 0 & 0\\ 0 & \lambda+2G & 0\\ 0 & 0 & G_t\end{bmatrix};\qquad \mathbf{D}_{yz}=\begin{bmatrix}0 & 0 & 0\\ 0 & 0 & \lambda_t\\ 0 & G_t & 0\end{bmatrix}$$

$$\mathbf{D}_{zx}=\begin{bmatrix}0 & 0 & G_t\\ 0 & 0 & 0\\ \lambda_t & 0 & 0\end{bmatrix};\qquad \mathbf{D}_{zy}=\begin{bmatrix}0 & 0 & 0\\ 0 & 0 & G_t\\ 0 & \lambda_t & 0\end{bmatrix};\qquad \mathbf{D}_{zz}=\begin{bmatrix}G_t & 0 & 0\\ 0 & G_t & 0\\ 0 & 0 & D_t\end{bmatrix}$$

Appendix II: Thin-layer matrices for cross-anisotropic materials

a) Linear expansion

The shape functions for this case are

$$N_1=\zeta;\qquad N_2=1-\zeta,\qquad \zeta=z/h$$

where $z=0$ at the bottom surface of the thin-layer and $z=h$ at the top surface. Evaluation of Eqs. (16a-d) results in the following thin-layer matrices:

$$\mathbf{M}=\frac{\rho h}{6}\begin{bmatrix}2\mathbf{I} & \mathbf{I}\\ \mathbf{I} & 2\mathbf{I}\end{bmatrix}$$

$$\mathbf{A}_{\alpha\alpha}=\frac{h}{6}\begin{bmatrix}2\mathbf{D}_{\alpha\alpha} & \mathbf{D}_{\alpha\alpha}\\ \mathbf{D}_{\alpha\alpha} & 2\mathbf{D}_{\alpha\alpha}\end{bmatrix},\qquad (\alpha=x,y)$$

$$\mathbf{A}_{xy}=\frac{h}{6}\begin{bmatrix}2\left(\mathbf{D}_{xy}+\mathbf{D}_{yx}\right) & \left(\mathbf{D}_{xy}+\mathbf{D}_{yx}\right)\\ \left(\mathbf{D}_{xy}+\mathbf{D}_{yx}\right) & 2\left(\mathbf{D}_{xy}+\mathbf{D}_{yx}\right)\end{bmatrix}$$

$$\mathbf{B}_{\alpha}=\frac{1}{2}\left(\begin{bmatrix}-\mathbf{D}_{\alpha z} & \mathbf{D}_{\alpha z}\\ -\mathbf{D}_{\alpha z} & \mathbf{D}_{\alpha z}\end{bmatrix}-\begin{bmatrix}-\mathbf{D}_{z\alpha} & -\mathbf{D}_{z\alpha}\\ \mathbf{D}_{z\alpha} & \mathbf{D}_{z\alpha}\end{bmatrix}\right),\qquad (\alpha=x,y)$$

$$\mathbf{G}=\frac{1}{h}\begin{bmatrix}\mathbf{D}_{zz} & -\mathbf{D}_{zz}\\ -\mathbf{D}_{zz} & \mathbf{D}_{zz}\end{bmatrix}$$

The matrices $\mathbf{D}_{\alpha\beta}$ used herein are defined in Appendix I. After assembling the elementary matrix $\mathbf{B}_\alpha$, the elementary matrix $\tilde{\mathbf{B}}_\alpha$ is obtained by changing the sign of every third column of $\mathbf{B}_\alpha$.

b) Quadratic expansion

The shape functions are now

$$N_1 = \zeta(2\zeta - 1), \qquad N_2 = 4\zeta(1-\zeta), \qquad N_3 = (1-\zeta)(1-2\zeta), \qquad \zeta = z/h$$

where again $z = 0$ at the bottom surface of the thin-layer and $z = h$ at its top surface. Evaluation of Eqs. (16a-d) results in the following elementary matrices:

$$\mathbf{M} = \frac{\rho h}{30}\begin{bmatrix} 4\mathbf{I} & 2\mathbf{I} & -\mathbf{I} \\ 2\mathbf{I} & 16\mathbf{I} & 2\mathbf{I} \\ -\mathbf{I} & 2\mathbf{I} & 4\mathbf{I} \end{bmatrix}$$

$$\mathbf{A}_{\alpha\alpha} = \frac{h}{30}\begin{bmatrix} 4\mathbf{D}_{\alpha\alpha} & 2\mathbf{D}_{\alpha\alpha} & -\mathbf{D}_{\alpha\alpha} \\ 2\mathbf{D}_{\alpha\alpha} & 16\mathbf{D}_{\alpha\alpha} & 2\mathbf{D}_{\alpha\alpha} \\ -\mathbf{D}_{\alpha\alpha} & 2\mathbf{D}_{\alpha\alpha} & 4\mathbf{D}_{\alpha\alpha} \end{bmatrix} \quad (\alpha = x, y)$$

$$\mathbf{A}_{xy} = \frac{h}{30}\begin{bmatrix} 4(\mathbf{D}_{xy} + \mathbf{D}_{yx}) & 2(\mathbf{D}_{xy} + \mathbf{D}_{yx}) & -(\mathbf{D}_{xy} + \mathbf{D}_{yx}) \\ 2(\mathbf{D}_{xy} + \mathbf{D}_{yx}) & 16(\mathbf{D}_{xy} + \mathbf{D}_{yx}) & 2(\mathbf{D}_{xy} + \mathbf{D}_{yx}) \\ -(\mathbf{D}_{xy} + \mathbf{D}_{yx}) & 2(\mathbf{D}_{xy} + \mathbf{D}_{yx}) & 4(\mathbf{D}_{xy} + \mathbf{D}_{yx}) \end{bmatrix}$$

$$\mathbf{B}_\alpha = \frac{1}{6}\left(\begin{bmatrix} 3\mathbf{D}_{\alpha z} & -4\mathbf{D}_{\alpha z} & \mathbf{D}_{\alpha z} \\ 4\mathbf{D}_{\alpha z} & \mathbf{0} & -4\mathbf{D}_{\alpha z} \\ -\mathbf{D}_{\alpha z} & 4\mathbf{D}_{\alpha z} & -3\mathbf{D}_{\alpha z} \end{bmatrix} - \begin{bmatrix} 3\mathbf{D}_{z\alpha} & 4\mathbf{D}_{z\alpha} & -\mathbf{D}_{z\alpha} \\ -4\mathbf{D}_{z\alpha} & \mathbf{0} & 4\mathbf{D}_{z\alpha} \\ \mathbf{D}_{z\alpha} & -4\mathbf{D}_{z\alpha} & -3\mathbf{D}_{z\alpha} \end{bmatrix}\right) \quad (\alpha = x, y)$$

$$\mathbf{G} = \frac{1}{3h}\begin{bmatrix} 7\mathbf{D}_{zz} & -8\mathbf{D}_{zz} & \mathbf{D}_{zz} \\ -8\mathbf{D}_{zz} & 16\mathbf{D}_{zz} & -8\mathbf{D}_{zz} \\ \mathbf{D}_{zz} & -8\mathbf{D}_{zz} & 7\mathbf{D}_{zz} \end{bmatrix}$$

Again, after assembling the elementary matrix $\mathbf{B}_\alpha$, the elementary matrix $\tilde{\mathbf{B}}_\alpha$ is obtained by changing the sign to every third columns of $\mathbf{B}_\alpha$.

Appendix III: Point load, Fourier integrals in k_y

The Fourier inversion of the point load solution over k_y is rather cumbersome, but is included here for the sake of completeness.

$$r=\sqrt{x^2+y^2}\,, \qquad \cos\theta=\frac{x}{r}, \qquad \sin\theta=\frac{y}{r} \qquad (\theta\neq\vartheta!!!)$$

Also $\sqrt{k_j^2-k_y^2}=-\mathrm{i}\sqrt{k_y^2-k_j^2}$ (because $\operatorname{Im}k_j<0$)

so

$$I_1=\frac{1}{2\mathrm{i}}\frac{1}{2\pi}\int_{-\infty}^{\infty}\frac{\mathrm{e}^{-\mathrm{i}|x|\sqrt{k_j^2-k_y^2}}}{\sqrt{k_j^2-k_y^2}}\mathrm{e}^{-\mathrm{i}k_y y}dk_y=\frac{1}{2}\frac{1}{2\pi}\int_{-\infty}^{\infty}\frac{\mathrm{e}^{-|x|\sqrt{k_y^2-k_j^2}}}{\sqrt{k_y^2-k_j^2}}\mathrm{e}^{-\mathrm{i}k_y y}dk_y=\frac{1}{4i}H_0^{(2)}\left(k_j r\right)$$

$$\boxed{I_1=\frac{1}{4i}H_0^{(2)}\left(k_j r\right)}$$

$$I_2=\frac{1}{2\pi}\int_{-\infty}^{\infty}\frac{k_y}{k_j^2}\frac{\operatorname{sgn}(x)}{2\mathrm{i}}\left(\mathrm{e}^{-\mathrm{i}|x|\sqrt{k_j^2-k_y^2}}-\mathrm{e}^{-|k_y x|}\right)\mathrm{e}^{-\mathrm{i}k_y y}dk_y$$

$$=\frac{1}{2k_j^2}\left\{\frac{1}{2\pi}\int_{-\infty}^{\infty}\operatorname{sgn}(x)\left(-\mathrm{i}k_y\right)\mathrm{e}^{-\mathrm{i}|x|\sqrt{k_j^2-k_y^2}}\,\mathrm{e}^{-\mathrm{i}k_y y}dk_y-\frac{1}{2\pi}\operatorname{sgn}(x)\int_{-\infty}^{\infty}\left(-\mathrm{i}k_y\right)\mathrm{e}^{-|k_y x|}\,\mathrm{e}^{-\mathrm{i}k_y y}dk_y\right\}$$

but

$$\frac{1}{2\pi}\int_{-\infty}^{\infty}\operatorname{sgn}(x)\left(-\mathrm{i}k_y\right)\mathrm{e}^{-\mathrm{i}|x|\sqrt{k_j^2-k_y^2}}\,\mathrm{e}^{-\mathrm{i}k_y y}dk_y=\frac{\partial^2}{\partial x\partial y}\frac{1}{2\pi}\int_{-\infty}^{\infty}\frac{\mathrm{e}^{-\mathrm{i}|x|\sqrt{k_j^2-k_y^2}}}{(-\mathrm{i})\sqrt{k_j^2-k_y^2}}\mathrm{e}^{-\mathrm{i}k_y y}dk_y=-\frac{\partial^2}{\partial x\partial y}\frac{1}{2\pi}\int_{-\infty}^{\infty}\frac{\mathrm{e}^{-|x|\sqrt{k_y^2-k_j^2}}}{\sqrt{k_y^2-k_j^2}}\mathrm{e}^{-\mathrm{i}k_y y}dk_y$$

$$=-\frac{1}{2\mathrm{i}}\frac{\partial^2 H_0^{(2)}\left(k_j r\right)}{\partial x\,\partial y}=-\frac{1}{2\mathrm{i}}\frac{\partial}{\partial y}\left[\frac{\partial H_0^{(2)}\left(k_j r\right)}{\partial r}\frac{\partial r}{\partial x}\right]=\frac{1}{2\mathrm{i}}\frac{\partial}{\partial y}\left[k_j H_1^{(2)}\left(k_j r\right)\frac{x}{r}\right]=\frac{k_j x}{2\mathrm{i}}\frac{\partial}{\partial r}\left[\frac{H_1^{(2)}\left(k_j r\right)}{r}\right]\frac{\partial r}{\partial y}$$

$$=\frac{k_j x}{2\mathrm{i}\,r^2}\left[r\frac{\partial}{\partial r}H_1^{(2)}\left(k_j r\right)-H_1^{(2)}\left(k_j r\right)\right]\frac{y}{r}$$

$$=\frac{k_j^2}{2\mathrm{i}}\frac{xy}{r^2}\left[\,H_0^{(2)}\left(k_j r\right)-2H_1^{(2)}\left(k_j r\right)/k_j r\right]$$

and

$$\operatorname{sgn}(x)\frac{1}{2\pi}\int_{-\infty}^{\infty}\left(-\mathrm{i}k_y\right)\mathrm{e}^{-|k_y x|}\,\mathrm{e}^{-\mathrm{i}k_y y}dk_y=\operatorname{sgn}(x)\frac{\partial}{\partial y}\frac{1}{2\pi}\int_{-\infty}^{\infty}\mathrm{e}^{-|k_y||x|}\,\mathrm{e}^{-\mathrm{i}k_y y}dk_y$$

$$=\operatorname{sgn}(x)\frac{\partial}{\partial y}\operatorname{Re}\left\{\frac{1}{\pi}\int_0^{\infty}\mathrm{e}^{-k_y|x|}\,\mathrm{e}^{-\mathrm{i}k_y y}dk_y\right\}$$

$$=\operatorname{sgn}(x)\frac{1}{\pi}\frac{\partial}{\partial y}\operatorname{Re}\frac{\mathrm{e}^{-k_y|x|}\,\mathrm{e}^{-\mathrm{i}k_y y}}{-|x|-\mathrm{i}y}\Bigg|_0^{\infty}=\operatorname{sgn}(x)\frac{1}{\pi}\frac{\partial}{\partial y}\operatorname{Re}\left(\frac{1}{|x|+\mathrm{i}\,y}\right)=\operatorname{sgn}(x)\frac{1}{\pi}\frac{\partial}{\partial y}\left(\frac{|x|}{r^2}\right)=-\frac{2}{\pi}\frac{xy}{r^4}$$

Hence

$$\boxed{I_2 = \frac{\cos\theta\sin\theta}{4\mathrm{i}}\left\{ H_0^{(2)}\left(Z_j\right) - \frac{2}{Z_j}\left(H_1^{(2)}\left(Z_j\right) - \frac{2\mathrm{i}}{\pi Z_j}\right)\right\}}, \qquad Z_j = k_j r\,, \qquad \sin\theta\,\cos\theta = \frac{xy}{r^2}$$

$$I_3 = \frac{1}{2\pi}\int_{-\infty}^{\infty}\frac{1}{2\mathrm{i}\,k_j^2}\left\{\sqrt{k_j^2 - k_y^2}\,\mathrm{e}^{-\mathrm{i}|x|\sqrt{k_j^2-k_y^2}} + \mathrm{i}\left|k_y\right|\mathrm{e}^{-|k_y x|}\right\}\mathrm{e}^{-\mathrm{i}k_y y}\,dk_y$$

$$= -\frac{1}{2}\frac{1}{k_j^2}\frac{\partial^2}{\partial x^2}\left[\frac{1}{2\pi}\int_{-\infty}^{\infty}\frac{\mathrm{e}^{-|x|\sqrt{k_y^2-k_j^2}}}{\sqrt{k_y^2-k_j^2}}\mathrm{e}^{-\mathrm{i}k_y y}\,dk_y\right] + \frac{1}{2k_j^2}\frac{1}{\pi}\mathrm{Re}\int_0^{\infty}\left\{k_y\,\mathrm{e}^{-k_y|x|}\right\}\mathrm{e}^{-\mathrm{i}k_y y}\,dk_y$$

$$= -\frac{1}{2}\frac{1}{k_j^2}\frac{\partial^2}{\partial x^2}\left[\frac{1}{2\mathrm{i}}H_0^{(2)}\left(k_j r\right)\right] + \frac{1}{2\pi}\frac{1}{k_j^2}\mathrm{sgn}\left(x\right)\frac{\partial}{\partial x}\mathrm{Re}\int_0^{\infty}\mathrm{e}^{-k_y|x|}\,\mathrm{e}^{-\mathrm{i}k_y y}\,dk_y$$

$$= -\frac{1}{4\mathrm{i}}\frac{1}{k_j^2}\frac{\partial}{\partial x}\left[\frac{x}{r}\frac{\partial}{\partial r}H_0^{(2)}\left(k_j r\right)\right] + \frac{1}{2\pi}\frac{1}{k_j^2}\frac{\partial}{\partial x}\left(\frac{x}{r^2}\right)$$

$$= -\frac{1}{4\mathrm{i}}\frac{1}{k_j^2}\left[\frac{\partial}{\partial x}\left(\frac{x}{r}\right)\frac{\partial H_0^{(2)}\left(k_j r\right)}{\partial r} + \left(\frac{x}{r}\right)^2\frac{\partial^2 H_0^{(2)}\left(k_j r\right)}{\partial r^2}\right] - \frac{1}{2\pi}\frac{1}{k_j^2 r^2}\left(1 - \frac{2x^2}{r^2}\right)$$

$$= -\frac{1}{4\mathrm{i}}\left[\frac{y^2}{r^2}\frac{1}{\left(k_j r\right)}\frac{\partial H_0^{(2)}\left(k_j r\right)}{\partial\left(k_j r\right)} + \left(\frac{x}{r}\right)^2\frac{\partial^2 H_0^{(2)}\left(k_j r\right)}{\partial\left(k_j r\right)^2}\right] - \frac{1}{2\pi}\frac{1}{\left(k_j r\right)^2}\frac{y^2 - x^2}{r^2}$$

$$= -\frac{1}{4\mathrm{i}}\left[\frac{y^2}{r^2}\frac{1}{Z}\frac{\partial H_0^{(2)}\left(Z\right)}{\partial Z} + \left(\frac{x}{r}\right)^2\frac{\partial^2 H_0^{(2)}\left(Z\right)}{\partial Z^2}\right] + \frac{1}{2\pi}\frac{1}{Z^2}\frac{x^2 - y^2}{r^2}$$

but

$$\frac{\partial^2}{\partial Z^2}H_0^{(2)}\left(Z_j\right) + \frac{1}{Z_j}\frac{\partial}{\partial Z_j}H_0^{(2)}\left(Z_j\right) + H_0^{(2)}\left(Z_j\right) = 0 \qquad \text{and} \qquad \frac{\partial}{\partial Z_j}H_0^{(2)}\left(Z_j\right) = -H_1^{(2)}\left(Z_j\right)$$

$$\boxed{I_3 = \frac{1}{4\mathrm{i}}\left[\cos^2\theta\,H_0^{(2)}\left(Z_j\right) - \frac{\cos^2\theta - \sin^2\theta}{Z_j}\left(H_1^{(2)}\left(Z_j\right) - \frac{2\mathrm{i}}{\pi Z_j}\right)\right]}$$

where

$$\cos^2\theta = \frac{x^2}{r^2}, \quad \sin^2\theta = \frac{y^2}{r^2}$$

$$I_4 = I_1 - I_3 = \frac{1}{4\mathrm{i}}H_0^{(2)}\left(Z_j\right) - \frac{1}{4\mathrm{i}}\left[\frac{x^2}{r^2}H_0^{(2)}\left(Z_j\right) - \frac{x^2 - y^2}{r^2}\frac{1}{Z_j}\left(H_1^{(2)}\left(Z_j\right) - \frac{2\mathrm{i}}{\pi Z_j}\right)\right]$$

$$\boxed{I_4 = \frac{1}{4\mathrm{i}}\left[\sin^2\theta\,H_0^{(2)}\left(Z_j\right) + \frac{\cos^2\theta - \sin^2\theta}{Z_j}\left(H_1^{(2)}\left(Z_j\right) - \frac{2\mathrm{i}}{\pi Z_j}\right)\right]}$$

$$I_5 = \frac{1}{2\pi}\int_{-\infty}^{\infty} \frac{\mathrm{sgn}(x)}{2\mathrm{i}\,k_j} \mathrm{e}^{-\mathrm{i}|x|\sqrt{k_j^2-k_y^2}}\, \mathrm{e}^{-\mathrm{i}k_y y} dk_y$$

$$= \frac{\mathrm{sgn}(x)}{2\mathrm{i}\,k_j} \frac{1}{2\pi}\int_{-\infty}^{\infty} \mathrm{e}^{-|x|\sqrt{k_y^2-k_j^2}}\, \mathrm{e}^{-\mathrm{i}k_y y} dk_y$$

$$= -\frac{1}{2\mathrm{i}\,k_j}\frac{\partial}{\partial x}\frac{1}{2\pi}\int_{-\infty}^{\infty} \frac{\mathrm{e}^{-|x|\sqrt{k_y^2-k_j^2}}}{\sqrt{k_y^2-k_j^2}} \mathrm{e}^{-\mathrm{i}k_y y} dk_y$$

$$= -\frac{1}{2\mathrm{i}\,k_j}\frac{\partial}{\partial x}\left(\frac{1}{2i} H_0^{(2)}\left(k_j r\right)\right) = \frac{1}{4k_j}\frac{\partial}{\partial r} H_0^{(2)}\left(k_j r\right)\frac{\partial r}{\partial x}$$

$$= -\frac{1}{4}\frac{x}{r} H_1^{(2)}\left(k_j r\right)$$

$$\boxed{I_5 = -\tfrac{1}{4}\cos\theta\, H_1^{(2)}\left(Z_j\right)}$$

$$I_6 = \frac{1}{2\pi}\int_{-\infty}^{\infty} \frac{k_y \mathrm{e}^{-\mathrm{i}|x|\sqrt{k_j^2-k_y^2}}}{2\mathrm{i}\,k_j\sqrt{k_j^2-k_y^2}} \mathrm{e}^{-\mathrm{i}k_y y} dk_y = \frac{1}{2k_j}\frac{1}{2\pi}\int_{-\infty}^{\infty} \frac{\left(-\mathrm{i}\,k_y\right)\mathrm{e}^{-|x|\sqrt{k_y^2-k_j^2}}}{\left(-\mathrm{i}\right)\sqrt{k_y^2-k_j^2}} \mathrm{e}^{-\mathrm{i}k_y y} dk_y$$

$$= \frac{\mathrm{i}}{2k_j}\frac{\partial}{\partial y}\frac{1}{2\pi}\int_{-\infty}^{\infty} \frac{\mathrm{e}^{-|x|\sqrt{k_y^2-k_j^2}}}{\sqrt{k_y^2-k_j^2}} \mathrm{e}^{-\mathrm{i}k_y y} dk_y$$

$$= \frac{\mathrm{i}}{2k_j}\frac{\partial}{\partial y}\left(\frac{1}{2\mathrm{i}} H_0^{(2)}\left(k_j r\right)\right) = \frac{1}{4k_j}\frac{\partial r}{\partial y}\frac{\partial}{\partial r}\left(H_0^{(2)}\left(k_j r\right)\right)$$

$$= -\frac{1}{4}\frac{y}{r} H_1^{(2)}\left(k_j r\right)$$

$$\boxed{I_6 = -\tfrac{1}{4}\sin\theta\; H_1^{(2)}\left(Z_j\right)}$$

$$I_7 = \frac{1}{2\pi}\int_{-\infty}^{\infty} \frac{1}{k_j}\frac{\mathrm{sgn}(x)}{2\mathrm{i}}\left(\mathrm{e}^{-\mathrm{i}|x|\sqrt{k_j^2-k_y^2}} - \mathrm{e}^{-|k_y x|}\right)\mathrm{e}^{-\mathrm{i}k_y y} dk_y$$

$$= I_5 - \frac{\mathrm{sgn}(x)}{2\mathrm{i}\,k_j}\frac{1}{\pi}\mathrm{Re}\int_0^{\infty} \mathrm{e}^{-k_y|x|}\, \mathrm{e}^{-\mathrm{i}k_y y} dk_y$$

$$= I_5 - \frac{\mathrm{sgn}(x)}{2\mathrm{i}\,k_j}\frac{1}{\pi}\mathrm{Re}\frac{1}{|x| + \mathrm{i}\,y} = I_5 - \frac{\mathrm{sgn}(x)}{2\mathrm{i}\,k_j}\frac{1}{\pi}\frac{|x|}{x^2+y^2}$$

$$= -\left\{\frac{1}{4}\frac{x}{r} k_j\, H_1^{(2)}\left(k_j r\right) + \frac{1}{2\mathrm{i}k_j}\frac{1}{\pi}\frac{x}{r^2}\right\}$$

$$\boxed{I_7 = -\tfrac{1}{4}\cos\theta\left(H_1^{(2)}\left(Z_j\right) - \frac{2\mathrm{i}}{\pi Z_j}\right)}$$

$$I_8 = \frac{1}{2\pi}\int_{-\infty}^{\infty} \frac{1}{2k_j\,\mathrm{i}} \left\{ \frac{k_y}{\sqrt{k_j^2 - k_y^2}}\, \mathrm{e}^{-\mathrm{i}|x|\sqrt{k_j^2-k_y^2}} - \mathrm{i}\,\mathrm{sgn}\left(k_y\right)\mathrm{e}^{-|k_y x|} \right\} \mathrm{e}^{-\mathrm{i}k_y y}\, dk_y$$

$$= I_6 - \frac{1}{2k_j}\frac{1}{2\pi}\int_{-\infty}^{\infty}\left[\mathrm{sgn}\left(k_y\right)\mathrm{e}^{-|k_y x|}\right]\mathrm{e}^{-\mathrm{i}k_y y}\, dk_y$$

$$= I_6 - \frac{1}{2k_j}\frac{\mathrm{i}}{\pi}\,\mathrm{Im}\int_0^{\infty}\mathrm{e}^{-k_y|x|}\,\mathrm{e}^{-\mathrm{i}k_y y}\, dk_y$$

$$= I_6 - \frac{1}{2k_j}\frac{\mathrm{i}}{\pi}\,\mathrm{Im}\frac{1}{|x| + \mathrm{i}\,y} = I_6 - \frac{1}{2k_j}\frac{\mathrm{i}}{\pi}\,\mathrm{Im}\frac{|x| - \mathrm{i}\,y}{x^2 + y^2}$$

$$= -\frac{1}{4}\frac{y}{r}H_1^{(2)}\left(k_j r\right) + \frac{1}{2k_j}\frac{\mathrm{i}}{\pi}\frac{y}{r^2}$$

$$\boxed{I_8 = -\tfrac{1}{4}\sin\theta\left\{H_1^{(2)}\left(Z_j\right) - \frac{2\mathrm{i}}{\pi Z_j}\right\}}$$

10. References

1. Haskell, N.A. (1953): "The dispersion of surface waves on multilayered media", *Bull. Seism. Soc. Am.*, **43** (1), 17-34
2. Hull [Seale], S. and Kausel, E. (1984): "Dynamic loads in layered halfspaces", *Proceedings, Fifth Engineering Mechanics Division Specialty Conference*, ASCE, I, 201-204, Laramie, Wyoming, August 1984.
3. Kausel, E. (1981): "An explicit solution for the Green's functions for dynamic loads in layered media", *MIT Research Report R81-13*, Department of Civil Engineering, MIT, Cambridge, MA 02139.
4. Kausel, E. and Roësset, J.M. (1981): "Stiffness matrices for layered soils", *Bull. Seism. Soc. Am.*, **71** (6), 1743-1761.
5. Kausel, E. and Peek, R. (1982): "Dynamic loads in the interior of a layered stratum: An explicit solution", *Bull. Seism. Soc. Am.*, **72** (5), 1459-1481 (see also Errata in *BSSA*, **74**, Aug. 1984. p. 1508).
6. Kausel, E. (1986): "Wave Propagation in Anisotropic Layered Media", *International Journal for Numerical Methods in Engineering*, **23**:1567 1578.
7. Kausel, E. (1988): "Local Transmitting Boundaries", Journal of Engineering Mechanics, ASCE, 114 (6):1011-1027.
8. Kausel, E. (1992): "Physical interpretation and stability of paraxial boundary conditions", Bulletin of the Seismological Society of America, 82(2): 898-913.
9. Kausel, E. (1994): "Thin-layer Method: Formulation in the time domain", *Int. J. Num. Meth. Eng.*, 37, 927-941.
10. Kausel, E. (2000): "The Thin-Layer Method in Seismology and Earthquake Engineering", *Wave Motion in Earthquake Engineering*, Chapter V, WIT Press, UK
11. Park, J. and Kausel, E. (2004) "Numerical dispersion in the thin-layer method", *Computers and Structures*, **82** , 607-625.
12. Kausel, E. (2006): *Fundamental Solutions in Elastodynamics: A Compendium*, Cambridge University Press, Cambridge, UK. See also the brief Corrigendum together

with an extensive Addendum at the following Internet address: "http://www.mit.edu/afs/athena.mit.edu/user/k/a/kausel/Public/webroot/articles/Green Functions/Fundamental Solutions, Corrigendum.pdf"

13. Lysmer, J. (1970): "Lumped mass method for Rayleigh waves", *Bull. Seism. Soc. Am.*, **43**, 17-34
14. Lysmer, J. and Waas, G. (1972): "Shear waves in plane infinite structures", *Journal of Engineering Mechanics*, ASCE, **98**, 85-105
15. Schmidt, H. and Tango, G. (1986): "Efficient global matrix approach to the computation of synthetic seismograms", *Geophys. J. R. Astr. Soc.*, **84**, 331-359
16. Seale, S. and Kausel, E. (1989): "Point loads in cross-anisotropic layered halfspaces", *Journal of Engineering Mechanics*, 115 (3): 509-542.
17. Tadeu, A. and Kausel, E. (2000): "Green's Functions for Two-and-a-Half Dimensional Elastodynamic problems", *Journal of Engineering Mechanics*, **126** (10), 1093-1097.
18. Thomson, W.T. (1950): "Transmission of elastic waves through a stratified soil medium", *J. Appl. Phys.*, **21**, 89-93
19. Waas, G. (1972): "Linear two-dimensional analysis of soil dynamic problems in semi-infinite layer media", PhD Thesis, University of California, Berkeley.